REPORT DOCUMENTATION PAGE

Form Approved
OMB No. 0704-0188

1. REPORT DATE (DD-MM-YYYY)	2. REPORT DATE	3. DATES COVERED (From - To)
18-07-2002	Final	01-10-2000 - 30-09-2001

4. TITLE AND SUBTITLE
Doping Mechanisms in Wide Bandgap Group III Nitrides

5a. CONTRACT NUMBER

5b. GRANT NUMBER
N00014-01-0012

5c. PROGRAM ELEMENT NUMBER

6. AUTHOR(S)
Wessels, Bruce W.

5d. PROJECT NUMBER

5e. TASK NUMBER

5f. WORK UNIT NUMBER

7. PERFORMING ORGANIZATION NAME(S) AND ADDRESS(ES)
Northwestern University
Materials Science & Engineering
2225 N. Campus Drive
Evanston, IL 60626-3108

8. PERFORMING ORGANIZATION REPORT NUMBER
RI

9. SPONSORING/MONITORING AGENCY NAME(S) AND ADDRESS(ES)
Office of Naval Research
Ballston Centre Tower One
800 N. Quincy Street
Arlington, VA 22217-5660

10. SPONSOR/MONITOR'S ACRONYM(S)
ONR

11. SPONSORING/MONITORING AGENCY REPORT NUMBER
N/A

12. DISTRIBUTION AVAILABILITY STATEMENT

DISTRIBUTION STATEMENT A
Approved for Public Release
Distribution Unlimited

13. SUPPLEMENTARY NOTES

14. ABSTRACT

The role of charge transfer and Fermi level position on impurity solubility, native defect formation and stability in GaN semiconductors was investigated. Several issues were addressed that include: (1) the structure, identity, solubility and stability of intentionally added and unintentional compensating donor defects in p-type and its material, (2) the role hydrogen complexes play in compensating p-type layers, and (3) the role oxygen and Si play in formation of defect complexes with Mg in GaN. The main objective was to determine the factors, which limit p-type conductivity in GaN and its alloys and to develop doping techniques to increase the hole concentrations to greater than 10^{19} cm^{-3}. The concentrations of both native defects and impurities were measured and its dependence on Fermi level determined. From the measured defect concentrations, the formation energies were calculated and compared to recent first principles, total-energy calculations for both native defects and impurities.

15. SUBJECT TERMS
Widegap semiconductor, doping studies, thin films

16. SECURITY CLASSIFICATION OF:			17. LIMITATION OF ABSTRACT	18. NUMBER OF PAGES	19a. NAME OF RESPONSIBLE PERSON
a. REPORT	b. ABSTRACT	c. THIS PAGE			Bruce W. Wessels
U	U	U	SAR		19b. TELEPHONE NUMBER (Include area code) (847) 491-3219

Standard Form 298 (Rev. 8-98)
Prescribed by ANSI-Std Z39-18

INSTRUCTIONS FOR COMPLETING SF 298

1. REPORT DATE. Full publication date, including day, month, if available. Must cite at lest the year and be Year 2000 compliant, e.g., 30-06-1998; xx-08-1998; xx-xx-1998.

2. REPORT TYPE. State the type of report, such as final, technical, interim, memorandum, master's theis, progress, quarterly, research, special, group study, etc.

3. DATES COVERED. Indicate the time during which the work was performed and the report was written, e.g., Jun 1997 - Jun 1998; 1-10 Jun 1996; May - Nov 1998; Nov 1998.

4. TITLE. Enter title and subtitle with volume number and part number, if applicable. On classified documents, enter the title classification in parentheses.

5a. CONTRACT NUMBER. Enter all contract numbers as they appear in the report, e.g. F33615-86-C-5169.

5b. GRANT NUMBER. Enter all grant numbers as they apperar in the report, e.g. 1F665702D1257.

5c. PROGRAM ELEMENT NUMBER. Enter all program element numbers as they appear in the report, e.g. AFOSR-82-1234.

5d. PROJECT NUMBER. Enter al project numbers as they appear in the report, e.g. 1F665702D1257; ILIR.

5e. TASK NUMBER. Enter all task numbers as they appear in the report, e.g. 05; RF0330201; T4112.

5f. WORK UNIT NUMBER. Enter all work unit numbers as they appear in the repor, e.g. 001; AFAPL30480105.

6. AUTHOR(S). Enter name(s) of person(s) responsible for writing the report, performing the research, or credited with the content of the report. The form of entry is the last name, first name, middle initial, and additional qualifiers separated by commas, e.g. Smith, Richard, Jr.

7. PERFORMING ORGANIZATION NAME(S) AND ADDRESS(ES). Self-explanatory.

8. PERFORMING ORGANIZATION REPORT NUMBER. Enter all unique alphanumeric report numbers assigned by the performing organization, e.g. BRL-1234; AFWL-TR-85-4017-Vol-21-PT-2.

9. SPONSORING/MONITORS AGENCY NAME(S) AND ADDRESS(ES). Enter the name and address of the orgazination(s) financially responsible for and monitoring the work.

10. SPONSOR/MONITOR'S ACRONYM(S). Enter, if available, e.g. BRL, ARDEC, NADC.

11. SPONSOR/MONITOR'S REPORT NUMBER(S). Enter report number as assigned by the sponsoring/ monitoring agency, if available, e.g. BRL-TR-829; -215.

12. DISTRIBUTION/AVAILABILITY STATEMENT. Use agency-mandated availability statements to indicate the public availability or distribution limitations of the report. If additional limitations/restrictions or special markings are indicated, follow agency authorization procedures, e.g. RD/FRD, PROPIN, ITAR, etc. Include copyright information.

13. SUPPLEMENTARY NOTES. Enter information not included elsewhere such as: prepared in cooperation with; translation of; report supersedes; old edition number, etc.

14. ABSTRACT. A brief (approximately 200 words) factual summary of the most significant information.

15. SUBJECT TERMS. Key words or phrases identifying major concepts in the report.

16. SECURITY CLASSIFICATION. Enter security classification in accordance with security classification regulations, e.g. U, C, S, etc. If this form contains classified information, stamp classification level on the top and bottom of this page.

17. LIMITATION OF ABSTRACT. This block must be completed to assign a distribution limitation to the abstract. Enter UU (Unclassified Unlimited) or SAR (Same as Report). An entry in this block is necessary if the abstract is to be limited.

Abstract

The role of charge transfer and Fermi level position on impurity solubility, native defect formation and stability in GaN semiconductors was investigated. Several issues were addressed that include: (1) the structure, identity, solubility and stability of intentionally added and unintentional compensating donor defects in p-type material, (2) the role hydrogen and its complexes play in compensating p-type layers, and (3) the role oxygen and Si play in formation of defect complexes with Mg in GaN. The main objective was to determine the factors, which limit p-type conductivity in GaN and its alloys and to develop doping techniques to increase the hole concentrations to greater than 10^{19} cm^{-3}. The concentrations of both native defects and impurities were measured and its dependence on Fermi level determined. From the measured defect concentrations, the formation energies were calculated and compared to recent first principles, total-energy calculations for both native defects and impurities.

Project Findings

Co-doping investigations:

The co-doping of GaN was investigated in order to understand the mechanism for the previously observed increase in p-type conductivity of epitaxial GaN. Two donor co-dopants were explored: Si and oxygen

The defect structure of oxygen-doped GaN grown by MOVPE was investigated. At high oxygen pressures, a super-linear increase of electron concentration as a function of partial pressure was observed. Electron concentrations as high as 7×10^{19} cm^{-3} were measured. Formation of micropits was observed by scanning electron microscopy in heavily doped samples. Cross-sectional transmission electron microscopy studies indicated the presence of epitaxial precipitates located on the cavity surface. The precipitates are believed to be related to gallium oxide. Using spatially resolved photoluminescence (PL), a broad PL band at 3.56 eV was observed near the micropit regions. The band was attributed to free-electron recombination from the highly degenerate areas associated with oxygen

Co-doping of p-type GaN with Mg and Si was investigated to determine its effect on deep level defect formation and luminescence. By co-doping with Si, the absolute intensity of the 2.8 eV blue luminescence band associated with deep donor-acceptor pair (DAP) recombination decreased by more than an order of magnitude. The observed decrease is attributed to the reduction of the concentration of nitrogen vacancy complexes that form deep donors. The dependence of the emission peak position on hole concentration was investigated. A blue shift was observed with increasing carrier concentration. The shift of the blue band with dopant concentration and excitation intensity is explained semi-quantitatively by a potential fluctuation model indicating it importance in DAP recombination.

Transition metal doping studies

The optical and electrical properties of Mn-doped epitaxial GaN were studied. Mn is believed to behave as an acceptor in GaN. Low-temperature optical absorption measurements indicate the presence of a Mn-related band with a well-resolved fine structure. The zero-phonon line is at 1.418±0.002 eV with a full width at half maximum of 20±1 meV. The pseudolocal vibrational modes associated with manganese were observed with energies of $h\nu_1$=20 and $h\nu_2$=73 meV. Deep level optical spectroscopy measurements on lightly Mn-doped samples indicate that Mn forms a deep acceptor level at E_v+1.42 eV. Using the vacuum referred binding energy model for transition metals and the measured Mn energy level, the electron affinity of GaN is calculated to be 3.4 eV, which agrees well with experimental values

Optical properties of a series of semi-insulating Mn-doped GaN co-doped with Mg were studied using photoluminescence (PL). A strong PL emission band at 1.0 eV was observed upon co-doping. The new band exhibited a rich fine structure with peaks at 1.057, 1.048, 1.035, 1.032, 1.020, 1.014, 1.008, 1.000 and 0.988±0.001 eV. The integrated and relative intensities of these lines varied as a function of the Mn concentration and excitation source. The measured luminescence decay time was 20-95 micros and depended on emission energy.

The optical absorption and photoluminescence spectra of semi-insulating Mn-doped GaN films were studied. Two characteristic bands were observed in the absorption spectra of Mn-doped epilayers at 300 K. The integrated intensities of these bands increased with increasing Mn concentration indicating that there were Mn-related. An analysis of the temperature behavior of the absorption band with a maximum at 1.5 eV indicated that it involved a free to bound transition from the valence band to the deep Mn-acceptor level. Photoluminescence measurements of Mn-doped films indicated the presence of an intra 3d-shell transition of the Mn ion. The luminescence band at 1.25±0.02 eV is tentatively attributed to the $^4T_1(G) \rightarrow {}^6A_1(S)$ transition.

These Mn doped GaN films may have potential as high temperature ferromagnetic semiconductors.

Personnel

Bing Han, a first year graduate student in Materials Science and Engineering, was supported on this project. Joel Gregie a third year graduate fellow was also partially supported.

Publications acknowledging ONR support

"Investigation of the defect structure of GaN heavily doped with oxygen," R.Y. Korotkov, F. Niu, J.M. Gregie, B.W. Wessels, Physica B 308-310 (2001).

"Optical Study of GaN: Mn co-doped with Mg grown by metal organic vapor phase epitaxy," R.Y. Korotkov, J.M. Gregie, B. Han, B.W. Wessels, Physica B 308-310 (2001).

"Mn-related absorption and PL bands in GaN grown by metal organic vapor phase epitaxy," R.Y. Korotkov, J.M. Gregie, B.W. Wessels, Physica B 308-310 (2001).

"Optical properties of the deep Mn acceptor in GaN:Mn," R.Y. Korotkov, J.M. Gregie, B.W. Wessels, Applied Physics Letters 80, 10 (2002).

"Investigation of the blue emission band in compensated GaN:Mg codoped with Si," B Han, J.M. Gregie, B.W. Wessels, PRB (2002) submitted.

Attachments:

ELSEVIER

Physica B 308–310 (2001) 26–29

PHYSICA B

www.elsevier.com/locate/physb

Investigation of the defect structure of GaN heavily doped with oxygen

R.Y. Korotkov, F. Niu, J.M. Gregie, B.W. Wessels*

Department of Materials Science and Engineering and Materials Research Center, Northwestern University, 2225 N. Campus Drive, Evanston, IL 60208-3108, USA

Abstract

The defect structure of oxygen-doped GaN grown by MOVPE was investigated. At high oxygen pressures, a super-linear increase of electron concentration as a function of partial pressure was observed. Electron concentrations as high as $7 \times 10^{19}\,cm^{-3}$ were measured. Formation of micropits was observed by scanning electron microscopy in heavily doped samples. Cross-sectional transmission electron microscopy studies indicated the presence of epitaxial precipitates located on the cavity surface. The precipitates are believed to be related to gallium oxide. Using spatially resolved photoluminescence (PL), a broad PL band at 3.56 eV was observed near the micropit regions. The band was attributed to free-electron recombination from the highly degenerate areas associated with oxygen.

Keywords: O-doped GaN; Microcavities; Photoluminescence

1. Introduction

Oxygen is known as a potential source of residual donors in GaN, although its doping behavior is not well understood [1–4]. The electrical properties of oxygen donors in GaN are somewhat controversial. Ionization energy values have ranged from 4 to 75 meV as determined by Hall-effect and optical measurements [1,5–8]. This large variation can be partially attributed to difficulties in their determination from Hall effect, presumably due to sample dopant inhomogeneities. A low temperature-conductivity tail is observed even in moderately doped GaN:O [8,9], which complicates calculations. Two possible explanations that account for this effect are the presence of a high conductivity layer at the layer substrate interface [10] or the formation of an impurity band [7]. SIMS studies corroborate the former model, since large concentrations of oxygen were observed within the first micron of the GaN film [11].

While it is now generally believed that oxygen is the shallow donor often responsible for the high residual background n-type conductivity in GaN, there are still unanswered questions regarding its incorporation. For example, we previously demonstrated that the electron concentration, n, increased with increasing partial pressure of oxygen as the square root from 1×10^{17} to $8 \times 10^{18}\,cm^{-3}$ [8]. However, it was also observed that the electron concentration increased super-linearly at higher oxygen partial pressures. In this paper, we present structural, optical, and electrical characterization of heavily oxygen-doped epilayers. Hexagonal surface microcavities (micropits) are formed on the surface of heavily oxygen-doped samples with $n > 10^{19}\,cm^{-3}$. Spatially resolved photoluminescence (PL) data provide evidence that the observed emission band at 3.56 eV is associated with oxygen doping and the presence of micropits.

2. Experimental

Oxygen-doped GaN epilayers were grown by MOVPE, as described elsewhere [8]. In brief, after deposition of the GaN buffer layer at 600°C, the

*Corresponding author. Tel.: +1-847-491-3537; fax: 1-847-491-7820.

E-mail address: b-wessels@northwestern.edu (B.W. Wessels).

0921-4526/01/$ - see front matter
PII: S0921-4526(01)00658-5

temperature was ramped to 1060°C and 50 nm of undoped GaN was deposited. This step was followed by the deposition of 2 μm of oxygen-doped GaN. Scanning electron microscopy (SEM) images were taken using a Hitachi S-4500 microscope. Typical operating conditions were 5–20 kV, with a magnification of 50–30,000 ×. High-resolution TEM was carried out with a Hitachi HF-2000 cold field emission microscope operating at 200 kV. The PL measurement setup was previously described [12]. He–Cd laser excitation was used. For spatially resolved measurements, the laser was focussed to a spot size of 20 μm.

Table 1
Electrical properties of GaN:O films

Sample	P (O_2) (Pa)	T (K)	NH_3 (sccm)	$n \times 10^{18}$ (cm^{-3})
RK120	0	1333	1400	0.1
RK216	0.4	1333	1400	1.8
RK213	6.2	1333	1400	16
RK217	12.1	1333	1400	29
RK234	10.3	1333	940	20
RK232	10.3	1273	1400	61
JG125 (GaN:Si)	0	1333	1400	30

3. Results and discussion

The surface morphology of deliberately oxygen-doped GaN was investigated. The surface of as-grown, undoped GaN films as seen in Fig. 1(a) is featureless when grown at high temperatures (1000–1070°C). As the partial pressure of oxygen is increased, the surface morphology remains unchanged for carrier concentration $<10^{19}\,cm^{-3}$. At this concentration, hexagonal-shaped microcavities are formed on the surface, as seen in Figs. 1(b) and (c). The concentration of the pits increased with free electron concentration, as seen by comparing Figs. 1(b) and (c), indicating that the formation of these surface microcavities was oxygen-related. The surface of the oxygen-doped sample with a RT electron concentration of $7 \times 10^{19}\,cm^{-3}$ was rough and completely covered with pits. A high-magnification SEM image of one of the microcavities is shown in Fig. 1(d).

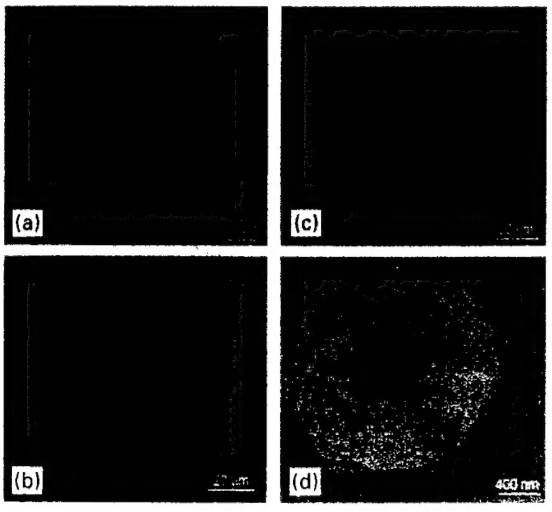

Fig. 1. SEM planar view image of oxygen-doped samples with (a) $n = 8 \times 10^{18}$, (b) 2.1×10^{19}, (c) $1.1 \times 10^{19}\,cm^{-3}$ and (d) high-resolution image of the pit.

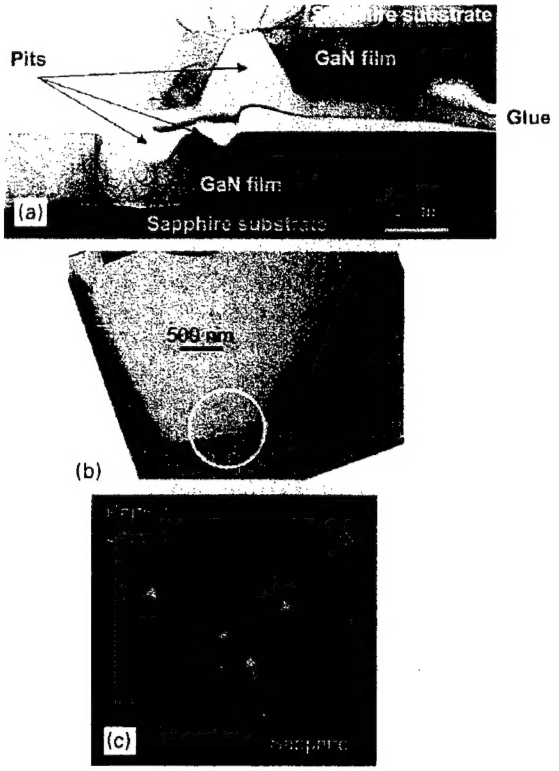

Fig. 2. (a) XTEM micrograph of GaN films grown on sapphire showing O-doping induced pits, (sample RK234, $n = 2 \times 10^{19}\,cm^{-3}$); (b) high-resolution XTEM image of a deep pit, with visible precipitate formation on the sidewalls; (c) SAD pattern of circled region of (b) that includes the Al_2O_3/GaN/ particle interface.

To determine the structure of the microcavities, TEM studies of highly oxygen-doped layers were conducted. A cross-sectional micrograph of a highly oxygen-doped sample RK234 (see Table 1) is shown in Fig. 2(a). It shows two pieces of a GaN sample grown on sapphire attached to each other by glue introduced during TEM sample preparation. Several pits are evident at the

surface of the GaN films. The depth of the pits varied, with some pits originating at the buffer layer surface. At the same time, several pits that nucleated during later stages of the GaN growth were also observed. Interestingly, a new epitaxial compound in the form of grains was observed on the pit surface (Fig. 2(b)). The structure of these grains was analyzed and compared to bulk GaN using selective area diffraction (SAD) patterns as shown in Fig. 2(c). Based on the fact that the SAD pattern of the grain regions was aligned in the same crystallographic direction as the GaN, it was concluded that these grains formed a textured epitaxial arrangement with GaN. The detailed work will be published elsewhere [13,14]. However, as to the identification of this second phase, we propose that it is likely a gallium oxide phase such as Ga_2O_3 or GaN_xO_{1-x}. The formation of a second phase of oxide at high partial pressures of oxygen is predicted from thermodynamic calculations [3]. The present study indicates that the solubility limit of oxygen in epitaxial GaN is of the order of $1 \times 10^{19}\,cm^{-3}$.

PL measurements at 20 K were conducted on heavily oxygen-doped GaN layers to determine whether or not oxygen introduces radiative centers. The samples studied are summarized in Table 1. A PL spectrum of a moderately O-doped sample (RK216) is shown in Fig. 3 for comparison. It consists of a strong donor-bound exciton (DBE) (FWHM = 5 meV) PL band located at 3.482 eV with a smaller shoulder of the free exciton (FE) at 3.49 eV, and so-called two-electron transitions at 3.458 and 3.463 eV, respectively. The exciton transitions are assigned by comparing their temperature-quenching behavior, and are in line with earlier results [5]. In heavily oxygen-doped samples, two DBEs were observed as shown in Fig. 3. The most intense exciton transition was at 3.482 eV for O-doped samples with $n < 1 \times 10^{19}\,cm^{-3}$, and at 3.472 eV for the samples with higher electron concentrations. Since the intensity ratio of the DBE transition at 3.482 eV to the FE transition was independent of partial pressure of oxygen, it was concluded that it did not involve an oxygen-bound exciton. In contrast, the relative PL intensity of the 3.472 eV DBE to the FE peak increased with partial pressure of oxygen as seen in Fig. 3. Therefore, we attribute the PL peak at 3.472 eV to an oxygen-related bound exciton.

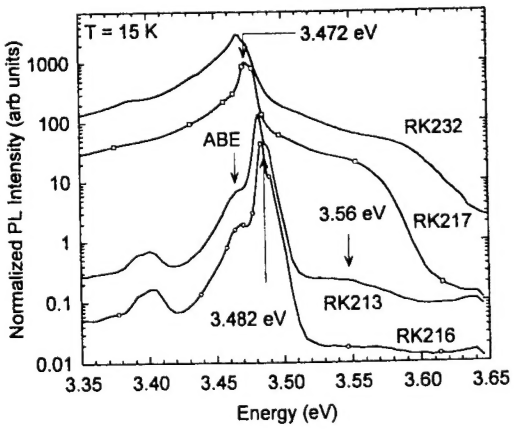

Fig. 3. PL spectra of oxygen-doped and undoped samples at 20 K. Two DBEs transitions are shown with arrows for the sample grown with different oxygen partial pressures (see Table 1).

The PL spectrum of a highly oxygen-doped ($2 \times 10^{19}\,cm^{-3}$) sample also exhibited a broad band extending to energies above the band gap in addition to the FE, DBE and ABE transitions. The band was observed above band gap as a shoulder to the FE and DBE transitions at 3.56 eV, as seen in Figs. 3 and 4. The intensity of this band increased with increasing partial pressure of oxygen, indicating that it was sensitive to the incorporation of oxygen in the film. As seen from this figure, the 3.56 eV band broadened when the electron concentration was increased (Table 1). However, no separate peak was observed, even at the highest electron concentration (RK232). The 3.56 eV band was only observed in heavily O-doped samples with electron concentrations higher than $10^{19}\,cm^{-3}$. We propose that the 3.56 eV band observed in highly oxygen-doped samples is due to free electron recombination.

To identify the origin of this band in highly oxygen-doped samples, spatially resolved PL experiments were conducted.[1] It can be seen in Fig. 4 that the intensity of the 3.56 eV band is higher in the pit regions than in nearly pit-free areas. Therefore, the 3.56 eV band PL is associated with the regions covered by hexagonal pits. The degenerate regions are formed in the vicinity of the hexagonal pits in agreement with spatially resolved PL, SEM, TEM and SIMS data. A similar broad, asymmetric band was previously observed in HVPE-grown, undoped GaN. In that case, it was related to localized degenerate regions using spatially resolved cathodoluminescence [15].

4. Conclusions

In this work, we have presented a study of heavily oxygen-doped GaN films grown by MOVPE. For higher electron donor concentrations, $n > 10^{19}\,cm^{-3}$, the formation of surface microcavities or micropits was observed. The pits were associated with oxide microprecipitates. These studies indicate that the solubility of oxygen in GaN is limited by the formation of Ga_2O_3-

[1] Hexagonal shaped pits and clusters can be observed with the help of optical microscopy. The He–Cd laser beam was focused ($d \sim 20\,\mu m$) both on the nearly pit-free regions (b in Fig. 4) and pit-clusters (a in Fig. 4).

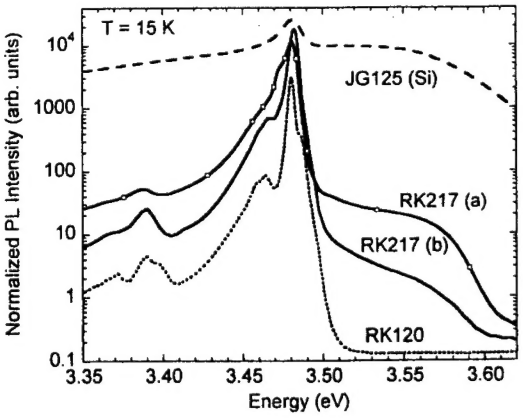

Fig. 4. LT PL spectra of nearly pit-free (RK217a) and pit-covered (RK217b) surface of highly oxygen-doped ($2.9 \times 10^{19}\,cm^{-3}$) sample. The spectra of an undoped sample (RK120) and a highly Si-doped sample (JG125) are shown for comparison.

related precipitates. Using spatially resolved PL measurements, these micropit regions were correlated with the 3.56 eV band due to free electron recombination in degenerate regions. These structural defects are likely responsible for the low mobility of the highly oxygen-doped layers.

Acknowledgements

This work is supported by the Office of Naval Research under grant N00014-01-0012.

References

[1] M. Illegems, H.C. Montgomery, J. Phys. Chem. Solids 34 (1973) 885.
[2] B.-C. Chung, M. Gershenzon, J. Appl. Phys. 72 (1992) 651.
[3] C.G. van de Walle, C. Stampfl, J. Neugerbauer, J. Crystal Growth. 195 (1998) 314.
[4] C. Wetzel, T. Suski, J.W. Ager III, E.R. Weber, E.E. Haller, S. Fischer, B.K. Meyer, R.J. Molnar, P. Perlin, Phys. Rev. Lett. 78 (1997) 3923.
[5] R. Niebuhr, K.H. Bachen, U. Kaufmann, M. Maier, C. Mertz, et al., J. Electron. Mat. 26 (1997) 1127.
[6] J.C. Zolper, R.G. Wilson, S.J. Pearton, R.A. Stall, Appl. Phys. Lett. 68 (1996) 1945.
[7] M.A. di Forte-Poisson, F. Huet, A. Roman, M. Tordjman, et al., J. Crystal Growth 195 (1998) 314.
[8] R.Y. Korotkov, B. Wessels, MRS Internet J. Nitride Semicond. Res. 5S1 (2000) W380.
[9] W. Gotz, R.S. Kern, C.H. Chen, H. Liu, D.A. Steigerwald, Mat. Sci. Eng. B59 (1999) 211.
[10] D.C. Look, R.J. Molnar, Appl. Phys. Lett. 70 (1997) 3377.
[11] G. Popovici, W. Kim, A. Botchkarev, H.P. Tang, H. Morkoc, J. Solomon, Appl. Phys. Lett. 71 (1997) 3885.
[12] M.A. Reshchikov, F. Shahedipour, R.Y. Korotkov, M.P. Ulmer, B.W. Wessels, Physica B 273–274 (1999) 105.
[13] R.Y. Korotkov, F. Niu, B.W. Wessels, in preparation.
[14] P.J. Dean, J.D. Cuthbert, D.G. Thomas, R.T. Lynch, Phys. Rev. Lett. 18 (1967) 122.
[15] B. Arnaudov, T. Paskova, E.M. Goldys, R. Yakimova, S. Evtimova, I.G. Ivanov, A. Henry, B. Monemar, J. Appl. Phys. 85 (1999) 7888.

Submitted PRB

Investigation of the blue emission band in compensated GaN:Mg codoped with Si

B. Han, J. M. Gregie and B. W. Wessels*

Northwestern University

Department of Materials and Engineering and Materials Research Center

Evanston, IL 60208

June 11, 2002

Abstract

Codoping of p-type GaN with Mg and Si was investigated to determine its effect on deep level luminescence. By codoping with Si, the absolute intensity of the 2.8 eV blue luminescence band associated with deep donor-acceptor pair (DAP) recombination decreased by more than an order of magnitude. The observed decrease is attributed to the reduction of the concentration of nitrogen vacancy complexes that form deep donors. The dependence of the emission peak position on hole concentration was investigated. A blue shift was observed with increasing carrier concentration. The shift of the blue band with dopant concentration and excitation intensity is explained semiquantitatively by a potential fluctuation model indicating its importance in DAP recombination.

*b-wessels@northwestern.edu

Introduction

Bipolar doping in wide-band-gap semiconductors such as GaN is difficult because of compensation by native defects or impurities.[1,2] Although high conductivity *n*-type of GaN is readily achieved, *p*-type material is much more difficult to attain.[3] It has been shown that in *p*-type GaN compensation by hydrogen donors and by nitrogen vacancy donors are factors that lead to highly resistive material.[4] While hydrogen donors can be eliminated either by low energy electron beam irradiation (LEEBI)[3] or by a N_2-ambient thermal annealing above 900K[5], elimination of native donors, such as the nitrogen vacancy (V_N) and its complexes, remains a more serious problem and represents the "*doping limit*" of *p*-type GaN.[6,7]

To minimize the formation of deep donor defects in GaN, codoping with shallow donors has been proposed.[4,8] Theory predicts that the formation energy of charged defects and impurities, which determines their equilibrium concentration, depends on the Fermi level.[4] The level in turn can be controlled through codoping with appropriately charged impurities. An example of the effect of codoping is that of hydrogen in *p*-type GaN.[4,9,10] Incorporation of hydrogen during growth suppresses the formation of nitrogen vacancy donors.[4] The hydrogen can be subsequently removed by annealing at high temperatures in nitrogen, thus activating acceptors.[4] Nevertheless, compensation by native defects still limits the hole conductivity in GaN:Mg layers even after hydrogen codoping and removal.[7,11] Meanwhile, only under certain restrictive conditions (e.g. low formation energy of the hydrogen defect, low activation barriers to dissociate the H-impurity complex and high diffusivity of H atom) can hydrogen passivation be applied to suppress native defect compensation and increase free carrier concentration in wide-gap-semiconductors.[4]

Yamamoto *et al.* proposed that highly conductive *p*-type GaN can be achieved by deliberate simultaneous incorporation of *p*-type dopants and controlled amount of *n*-type dopants.[12] Several

studies have confirmed these predictions.[13-15] Korotkov et al. observed improved *p*-type conductivity upon oxygen donor codoping through a decrease of the acceptor (Mg) activation energy.[15] However, the different mechanisms by which the codoping method leads to high conductivity are not well-established and remain controversial. Indeed, using first principles total energy calculations, Zhang, *et al.* predicted that under thermal equilibrium neither higher solubility of desired (*p*-type) dopants nor shallower acceptor levels in semiconductors can be achieved by codoping.[16]

In this work Mg-doped GaN has been co-doped with the shallow donor Si to suppress the formation of native donors. Photoluminescence (PL) measurements were carried out on deliberately codoped material to determine the effect of shallow donor incorporation on deep donor-acceptor pair (DAP) luminescence associated with nitrogen vacancy complexes. Upon Si codoping, the intensity of the blue DAP band decreased by more than an order of magnitude. For heavily Si-doped, *n*-type films, the band is completely quenched. These results indicate that native defect formation can be efficiently suppressed by means of codoping the films with *n*-type dopants. This approach to defect control is generally applicable to wide-band-gap semiconductors.

Experimental details

Mg-doped and Mg-Si co-doped GaN films were grown by atmospheric pressure metal-organic vapor phase epitaxy (MOVPE) on c-phase sapphire substrates. Ammonia (NH_3) and trimethylgallium (TMGa) were used as reactants, and hydrogen was the carrier gas. The source materials for Mg and Si are bis(cyclopentadienyl)magnesium (Cp_2Mg) and a 100 ppm silane (SiH_4) mixture in H_2, respectively. Hydrogen is the carrier gas. For these studies a multi-layer structure was used. Film growth was initiated with a low temperature GaN buffer layer, followed by a 500 nm insulating, Mg-doped layer. The Mg-Si codoped layer, 0.5-1 μm thick, was

subsequently grown at 1030°C. The codoped films were annealed for 15 minutes in N_2 at 850°C to eliminate hydrogen.

Photoluminescence measurements were made between 17K and 350K using a closed-cycle He cryostat. The sample temperature was measured with a carbon temperature sensor and stabilized by a temperature controller at temperatures between 17K and 350K. A He-Cd laser (photon energy 3.81 eV) was used as an excitation source in the reflection configuration. The PL signal was dispersed by a 0.75m SPEX grating monochromator and detected by a Hamamatsu photomultiplier tube R928 and a photon counting system. The excitation intensity was varied over the range 10^{-5}-3.2 W/cm^2 using calibrated neutral density filters.

Van der Pauw measurements were conducted at room temperature. Either In or Ni/Au were used as contacts. The magnetic field was 3200 G. The applied currents were between 0.01 and 0.1mA.

Experimental results and discussions

1. The effect of codoping on PL intensity of the blue band

PL spectra for Mg-doped and Mg-Si co-doped films were measured at 17.5 K. At a high Mg concentration, a broad blue band peaked around 2.8 eV is observed in the Mg-doped GaN as shown in Fig. 1. The origin of the blue band was previously attributed to DAP emission involving a Mg_{Ga} acceptor and a nitrogen vacancy donor or related deep donor complex.[11,17,18]

To determine the effect of Si codoping on the blue band emission intensity in *p*-type GaN, a series of Mg-Si co-doped films were investigated grown with a constant Mg flow rate, while the flow rate of Si was varied. The growth conditions and the electrical characteristics for this series of films are summarized in Table I.

Fig. 1 shows the PL spectra for this series of co-doped samples at a constant excitation level. Since the maximum peak position of the blue band depends on temperature and excitation intensity, all the PL spectra in Fig. 1 were measured with an excitation density of 40 mW/cm^2. The excitation power was kept at a relatively low level to avoid saturation of the intensity. However, the intensities of the blue bands are high enough to allow comparison of the PL intensity among different samples.

The dominant emission band in the Si-Mg co-doped samples was also at 2.8 eV at 17.5 K. As shown in Fig. 1, the measured intensity of the blue band in *p*-type GaN decreased with increasing Si doping. Compared to a Mg-doped film grown under similar condition, but without Si, the absolute intensity of the blue band for *p*-type co-doped GaN decreased by more than an order of magnitude with Si codoping. When the Si dopant concentration was very high, the film converted to *n*-type. In that case, no blue band can be observed (as shown with a dotted line in Fig. 1) and a shallow DAP band with zero phonon line peaked at 3.27 eV dominates the spectrum. The quenching of the blue band is attributed to suppression of the deep native donor formation by incorporation of the shallow donor—Si, which will be discussed later.

To determine the nature of the defects involved in the blue band observed in codoped samples, the temperature dependence of the emission intensity was measured. The quenching of the PL intensity with increasing temperature for Mg-doped and Mg-Si co-doped *p*-type films is shown in Fig. 2. The blue band quenches in all three samples at temperatures above 150K. The quenching is attributed to the thermal release of trapped electrons from a deep donor state.[19] The temperature dependence of the blue band intensity can be fit using the equation:

$$I(T) = I_0 / [1 + A \exp(-E_D / kT)] \qquad (1)$$

where E_D is activation energy of the donor and A is taken to be a temperature independent constant. The measured activation energies for the samples are summarized in Table I. The quenching curves indicate that the thermal depth of the donor is 245±5 meV for all the epilayers studied. Consequently, the donors involved in the DAP emission band remain unchanged with Si codoping. This leads to the conclusion that donor responsible for the blue DAP emission is identical in the Mg-doped and Mg-Si codoped samples. Since the PL intensity decreases with increasing Si flow rate and the blue band dominates the low temperature PL spectrum for solely Mg-doped GaN, the donor cannot be attributed to the shallow donor Si_{Ga} or a Si related complex. Otherwise an increase of the blue band intensity, rather than decrease, should be observed with Si flow rate. The intensity quenching is therefore attributed to a decrease in the deep donor concentration.

It should be noted that similar concentration quenching was observed for codoping with shallow oxygen donors in GaN:Mg by Korotkov et al.[8] In that work, the absolute intensity of the blue band was also found to decrease with increasing oxygen incorporation. It was concluded that the oxygen donor plays no role in the blue DAP band.

The observed quenching of the blue band with addition of shallow donors is consistent with calculations for the native defect formation and the influence of Fermi energy reported by Van de Walle *et al.*[20] In these calculations, the formation energy of the compensating native donor increases with Fermi energy E_F, which in turn is increased by addition of shallow donors. This addition leads to the decrease of the concentration of native donors. Consequently, a decrease of the absolute intensity of the blue DAP band would be expected.[11] It is important to note that no blue band is observed in the *n*-type film. This is consistent with the high formation energy of the native donors in *n*-type samples.

Si is not highly diffusive in p-type GaN and cannot be eliminated as easily as hydrogen by post-growth treatment.[4] Therefore, in order to decrease the total concentration of donors in *p*-type GaN by codoping with Si, the reduction of the native donor (nitrogen vacancy or its complexes) concentration must be larger than the increase of Si concentration.

To determine quantitatively the effect of addition of Si on the reduction of deep donors, its dependence on Fermi level needs to be considered. The equilibrium concentration of the native defect $N_{D(V_N)}$ and its dependence on formation energy is given by $N_{D(V_N)} = N_{sites} \exp(-E^f / kT)$. The formation energy, E^f, in turn, is a function of the Fermi level:

$$E^f(GaN{:}V_N) = E_{tot}(GaN{:}V_N) + \mu_N + qE_F \qquad (2)$$

where E_{tot} is the formation energy of the neutral defect, E_F is the Fermi level, μ_N is the chemical potential, and q is the charge state of the defect. Generally, the Fermi energy of *p*-type GaN at growth condition (1300K) is within 0.3 eV of the top of the valence band.[21] According to theory,[20] the *3+* charge state is more stable than the *1+* charge state for V_N in this range.

The Fermi level can be increased by adding shallow donors. In highly compensated *p*-type GaN, the dependence of Fermi energy on Si donor incorporation is:[22]

$$dE_F = kT \frac{N_A}{(N_A - N_D)N_D} dN_{D(Si)} \qquad (3)$$

where N_A the concentration of acceptors, N_D the total concentration of donors and $N_{D(Si)}$ the concentration of Si in the GaN layer. For a large Si concentration, it is the dominating compensating defect in *p*-type GaN at 1300K,[4] $N_D \approx N_{D(Si)}$. When $N_A > N_D$, Eq. (3) reduces to $dE_F = kTd\ln(|N_{d(Si)}|)$. Combining Eq. (2) and (3), it follows that $N_{D(V_N)}$ decreases with E_F following:

$$dN_{D(V_N)} = \frac{1}{kT}[N_{sites}\exp(-E_f / kT)](-3dE_F) = -N_{D(V_N)}[3d|N_{D(Si)}|] \qquad (4)$$

Eq. (4) shows that $d\ln|N_{D(V_N)}| = -3d\ln|N_{D(Si)}|$. Consequently, when Si is incorporated into *p*-type GaN, the Fermi level increases and the reduction of $N_{d(V_N)}$ is more than the increase of $N_{d(Si)}$ because of the differences in charge states of nitrogen vacancy and Si in *p*-type GaN. Although Si cannot be removed after growth, codoping *p*-type GaN with Si can still improve electrical properties of the *p*-type material by reduction of deep donors.

A similar process can circumvent the problem of self-compensation by native defects in other wide-band-gap semiconductors as long as the dopant impurity (e.g. Si) is the dominating compensation defect at growth conditions and the charge state of native defects is larger than that of the impurity codopants.

2. Properties of the blue emission band in compensated p-type GaN.

The dependence of emission energy on excitation power of the blue band was studied in compensated *p*-type GaN to determine the role of potential fluctuations. Fig. 3 shows the PL peak shift of the blue band at room temperature as a function of excitation power for Mg-doped and Mg-Si codoped samples. A blueshift of the blue band with increasing excitation intensity has been consistently observed for all the p-type samples.

Although most groups agree that the blue band involves a DAP transition between a Mg acceptor and deep nitrogen vacancy donor, the reason why the emission peak energy varies for different samples is still controversial. The shift can be explained by the DAP nature of this transition,[18] or alternatively a model involving potential fluctuaions.[23] Colton et al. suggested that the peak energy of the blue band marks the transition from localized states to delocalized states within an

Urbach-type band tail.[24] All these explanations are qualitative. In this investigation, a quantitative model based on potential fluctuations is given to explain the shift of the blue emission peak energy.

In compensated and highly doped semiconductors, potential fluctuations are expected to strongly affect the optical properties due to the inhomogeneous distribution of charged defects.[19,25] Diagonal radiative transitions between holes localized in the "hills" of the valence band and electrons localized in the "valleys" of the conduction band reduce the recombination energy and redshift the PL band. The wide range of photon emission energies made possible by these potential fluctuation broadens the PL band. According to the model developed by Shklovskii and Efros,[25] when the impurities are randomly distributed, the average amplitude Γ of potential fluctuations for a p-type semiconductor depends on the total concentration of charged impurities ($N_T = N_A^- + N_D^+$) and the hole concentration p:

$$\Gamma = \frac{e^2}{4\pi\varepsilon\varepsilon_0} \cdot \frac{N_T^{2/3}}{p^{1/3}} \qquad (5)$$

In the presence of potential fluctuations, the blue DAP emission energy is thus given by[26]

$$E(\hbar\omega) = E_g - (E_D + E_A) - 2\Gamma = E_g - E_A - E_D - 2 \cdot \frac{e^2}{4\pi\varepsilon\varepsilon_0} \cdot \frac{(\frac{2N_A K}{K+p} - p)^{2/3}}{p^{1/3}} \qquad (6)$$

where E_g is the band gap and E_A and E_D are the acceptor and donor energies, respectively.K is defined in Ref. 26. As a result, when the excitation intensity increases, the band blueshifts as shown in Fig. 3 because of increased screening of the potential fluctuations by photogenerated carriers,. At the low excitation limit, no shift is observed. This can be explained by the fact that at low excitation intensity, photogenerated nonequilibrium carrier concentration is very low compared to equilibrium carrier concentration generated by thermal ionization. In this case, the

hole concentration in the films is essentially identical to that obtained by Hall effect measurements in the dark. The small change in carrier concentrations upon low-level photoexcitation leads to a negligible change of the potential fluctuation magnitude and no shift is observed.

The peak positions for two films (JG138 and JG142) at low excitation limit are close, indicating similar potential fluctuation amplitudes. Since the hole concentration of both films are around 3×10^{17} cm^{-3}, Eq. (6) indicates that the Mg doping density N_A is nearly the same for these samples even though Si dopant was increased.

To determine the amplitude Γ of the potential fluctuations, the energy of the main peak at the low excitation limit is plotted versus the cube root of the measured hole concentration in the epilayers at room temperature, as shown in Fig. 4a. The solid curve is calculated using Eq. (6) after assuming N_A is independent of Si dopant concentration. For these calculations, N_A is used as a fitting parameter and obtained by least square regression. The estimated value of N_A from the fit is 4.8×10^{19} cm^{-3}. From the Mg doping density N_A and measured hole concentration p, Γ can be calculated (Ref. 26). The potential fluctuations range from 0.072 to 0.141 eV as listed in Table 1. Using Eq. (6) the peak position of the blue band without any potential fluctuations is thus calculated to be 2.95 eV

After taking into account the effect of potential fluctuations, the activation energy of the acceptor involved in the blue band can be determined from Eq. (6) and is given as $E_A = E_g - \hbar\omega - E_D$, where the band gap E_g is taken as 3.42 eV at room temperature, and $\hbar\omega$ (2.95 eV) is the emission energy without potential fluctuations. E_D was previously determined from thermal quenching as 245±5 meV. The activation energy of the acceptor is, therefore, 225±5 meV. This further

supports the model that the blue band involves a transition from a deep donor to Mg_{Ga}; the ionization energy of the latter defect was reported to be between 200 and 290 meV.[3, 27,28]

While the relationship between peak position and hole concentration is well-described by Eq. (6) . nevertheless a linear dependence of the peak position of the blue band on the reciprocal of the hole concentration can also be used to describe the observed room temperature dependence, as indicated by Fig. 4 b. For a constant N_A, the magnitude of the potential fluctuation can be simplified to $\Gamma = S \times p^{-1}$, where $S = (2N_A K)^{2/3} e^2 / 4\pi\varepsilon\varepsilon_0 = 2.3 \times 10^{16} eV \cdot cm^{-3}$.[29] Consequently, the peak energy of the blue band in p-type GaN films depends linearly on the reciprocal of the hole concentration at room temperature following:

$$E(\hbar\omega) = E_g - (E_D + E_A) - 2S \times p^{-1} \qquad (7)$$

From a simple linear extrapolation of the data the peak position blueshifts to 2.96 eV when the potential fluctuation $\Gamma = S \times p^{-1}$ decreases to zero at $p^{-1} = 0$. This result is in agreement with the result of 2.95 eV previously obtained using Eq. (6).

Conclusions

In conclusion, codoping of *p*-type GaN with Mg and Si was investigated to determine its effect on deep level luminescence. The absolute intensity of the blue luminescence (DAP) band for Mg-doped *p*-type GaN is reduced by more than an order of magnitude with Si-codoping. The decrease is attributed to a decrease in the compensating native defects, V_N, in Mg-doped *p*-type GaN upon codoping of *n*-type dopants. Our result is consistent with density-functional theory calculations for the native defect formation and the influence of Fermi energy on defect stability in GaN. The blue shift of the blue DAP band was studied for the codoped films. The shift is

explained semiquantitatively by a potential fluctuation model. Potential fluctuations as large as 0.14 eV are observed in the compensated films.

Acknowledgements

This work is supported by an ONR grant under contract No. N00014-01-1-0012 (C. Wood, monitor) and by the National Defense Science and Engineering Graduate Fellowship (JMG) awarded by the Air Force and the Department of Defense.

References:

[1]G. Mandel, Phys. Rev. **134,** A1073 (1964).

[2]J. A. Van Vechten: *Handbook on Semiconductors*, ed. S. P. Keller (North Holland, Amsterdam, 1980) Vol. 3, Chap. 1.

[3]H. Amano, M. Kito, K. Hiramatsu, and I. Akasaki, Jpn. J. Appl. Phys., Part 2 **28,** L2112 (1989).

[4]J. Neugebauer and C. G. Van de Walle, Appl. Phys. Lett. **68,** 1829, (1998).

[5]S. Nakamura, T. Mukai, M. Senoh, and N. Iwasa, Jpn. J. Appl. Phys., Part 2 **31,** L139 (1992).

[6]S. B. Zhang, S.-H. Wei, and A. Zunger, Physica B, **273-274,** 976 (1999).

[7]U. Kaufmann, P. Schlotter, H. Obloh, K. Kohler, and M. Maier, Phys. Rev. B **62,** 10867 (2000).

[8]R.K. Korotkov, J.M. Gregie, and B.W. Wessels, Mat. Res. Soc. Symp., **639,** G6.39.1 (2001).

[9]S. Nakamura, N. Iwasa, M. Senoh, and T. Mukai, Jpn. J. Appl. Phys., Part 1 **31,** 1258 (1992).

[10]J. A. Van Vechten, J. D. Zook, R. D. Horning, and B. Goldenberg, Jpn. J. Appl. Phys. Part 1 **31,** 3662 (1992).

[11]F. Shahedipour and B. W.Wessels, Appl. Phys. Lett. **76,** 3011, (2000).

[12] T. Yamamoto, H. Katayama-Yoshida, and R. Kato, Jpn. J. Appl. Phys., Part 2 **36,** L180 (1997).

[13]O. Brandt, H. Yang, H. Kostial, and K.H. Ploog, Appl. Phys. Lett. **69,** 2707 (1996).

[14]S.Nakamura, et al., Application to Japanese Patent (Fabrication method of the *p*-type nitride compound semiconductors and nitride semiconductor devices: JP H8-296872 [Published in JP H10-154829]).

[15]R. Y. Korotkov, J. M. Gregie, and B. W. Wessels, Appl. Phys. Lett. **78,** 222 (2001).

[16]S.B. Zhang, S.-H. Wei, and Yanfa Yan, Physica B, **302-303,** 135 (2001).

[17]U. Kaufmann, M. Kunzer, M. Maier, H. Obloh, A. Ramakrishnan, B. Santic, and P. Schlotter, Appl. Phys. Lett. **72,** 1326 (1998).

[18]M. A. Reshchikov, G.-C. Yi, and B. Wessels, Phys. Rev. B **59,** 13176 (1999).

[19]M. Leroux, N. Grandjean, B. Beaumont, G. Nataf, F. Semond. J. Massies, and P. Gilbart, J. Appl. Phys., **86,** 3721 (1999).

[20]C.G. Van de Walle, Mat. Sci. Forum, **338-342,** 1561 (2000).

[21]H. Nakayama, P. Hacke, M.R.H. Khan, T. Detchprohm, K. Hiramatsu, and N. Sawaki, Jpn. J. Appl. Phys., Part 2, **35,** L282 (1996).

[22]J.S. Blakemore, *Semiconductor Statistics* (Dover, New York, 1987).

[23]E. Oh, H. Park, and Y. Park, Appl. Phys. Lett. **72,** 1326 (1998).

[24]J. S. Colton and P. Y. Yu, Appl. Phys. Lett. **78,** 2500 (2001).

[25]B.I. Shklovskii and A.L. Efros, *Electronic Properties of Doped Semiconductors* (Springer, Berlin, 1984).

[26]For *p*-type GaN, where the acceptors are incompletely ionized at room temperature and are compensated by native donors and *n*-type impurities, the relationship between total donor concentration N_D, Mg doping concentration N_A and equilibrium hole concentration p_0 is (Ref. 22)

$$\frac{p_0(p_0+N_D)}{(N_A-N_D-p_0)}=(\frac{N_v}{\beta})\exp(-E_A/kT)$$

where E_A is the thermal ionization energy, β is the spin degeneracy of the acceptors and N_v is the effective density of states in the valence band. The Fermi level in the *p*-type samples is well below the energy level of potential donor impurities. Therefore, virtually all the donors are ionized. Following the argument by Kaufmann (Ref. 7), at room temperature, β=3.6 and $K=(N_v/\beta)\exp(-E_A/kT)=1.8\times10^{16}\text{cm}^{-3}$. This leads to $N_D^+=N_D=KN_A/(K+p)-p$, where N_D^+ is the density of ionized donors. The electrical neutrality condition is $N_A^-=N_D^++p$ for *p*-

type material. Therefore, the total concentration of charged impurities is in the following form $N_T = N_A^- + N_D^+ = 2N_A K/(K+p) - p$, and the average potential depth can be rewritten as

$$\Gamma = \frac{e^2}{4\pi\varepsilon\varepsilon_0} \cdot \frac{(\frac{2N_A K}{K+p} - p)^{2/3}}{p^{1/3}}$$

Consequently, the blue band emission energy is given by

$$E(\hbar\omega) = E_g - (E_D + E_A) - 2\Gamma = E_g - E_A - E_D - 2 \cdot \frac{e^2}{4\pi\varepsilon\varepsilon_0} \cdot \frac{(\frac{2N_A K}{K+p} - p)^{2/3}}{p^{1/3}}$$

[27]M. Ilegems and R. Dingle, J. Appl. Phys. **44**, 4234 (1973).

[28]M.Smith, G.D. Chen, J.Y. Lin, H.X. Jiang, A. Salvador, B.N.Sverdlov, A. Sverdlov, A. Botchkarev, H. Morkoc, and B. Goldenberg, Appl. Phys. Lett. **68,** 1883 (1996).

[29]Since the value of $2N_A K/(K+p)$ is more than an order of magnitude larger than p in the films and p K, Γ can be combined as $\Gamma = \frac{e^2}{4\pi\varepsilon\varepsilon_0} \cdot \frac{(2N_A K/p)^{2/3}}{p^{1/3}} = S \times p^{-1}$, where $S = (2N_A K)^{2/3} e^2 / 4\pi\varepsilon\varepsilon_0 = 2.3 \times 10^{16}\, eV \cdot cm^{-3}$ is a constant.

Table I. Electronic characteristics of Mg doped and Si codoped samples

Sample No.	Mg (μmol /min)	Si (nmol /min)	p ($\times 10^{17}$cm^{-3})	ρ (Ωcm)	Activation energy of donor (eV)	Γ(eV)
JG 136	0.18	0	2.5	2.6	0.25	0.087
JG 138	0.18	0.28	3	1.8	N/A	0.072
JG 140	0.18	0.56	1.5	3.9	0.24	0.141
JG 141	0.18	1.12	2	3.2	0.25	0.107
JG 142	0.18	2.24	3	2.2	N/A	0.072
JG 148	0.09	4.48	55*	0.09	N/A	N/A

*-indicates *n*-type material.

Figure Captions:

Fig. 1. PL spectra for heavily Mg-doped and Si co-doped samples taken at 17.5 K and 40 mW/cm^2. The absolute intensity of the blue band in *p*-type GaN decreased steadily with increasing Si flow rate. The data shows that the band (dotted curve) is completely quenched in *n*-type material with over codoping of Si.

Fig. 2. Temperature dependence of the blue band emission intensity in Mg-doped and Si-codoped samples. Solid lines are fits based on Eq. (1). The calculated activation energy for donors in different samples is 245±5 meV.

Fig. 3. Dependence of the blue band peak position on excitation intensity at room temperature for the Mg-doped and Si-codoped samples. The peak shift is independent of excitation level at the low excitation limit. Note the peak positions of sample JG 138 and JG 148 are close at low excitation intensity.

Fig. 4.a Dependence of the peak energy of the blue band with the cube root of the free carrier concentration. The solid curve is the fit based on Eq. (6). The fitting parameter, N_A, is 4.8×10^{19} cm^{-3}. b, A linear dependence of the peak position of the blue band on the reciprocal of the hole concentration can also be used to describe the observed room temperature dependence as in Eq. (7).

Fig. 1

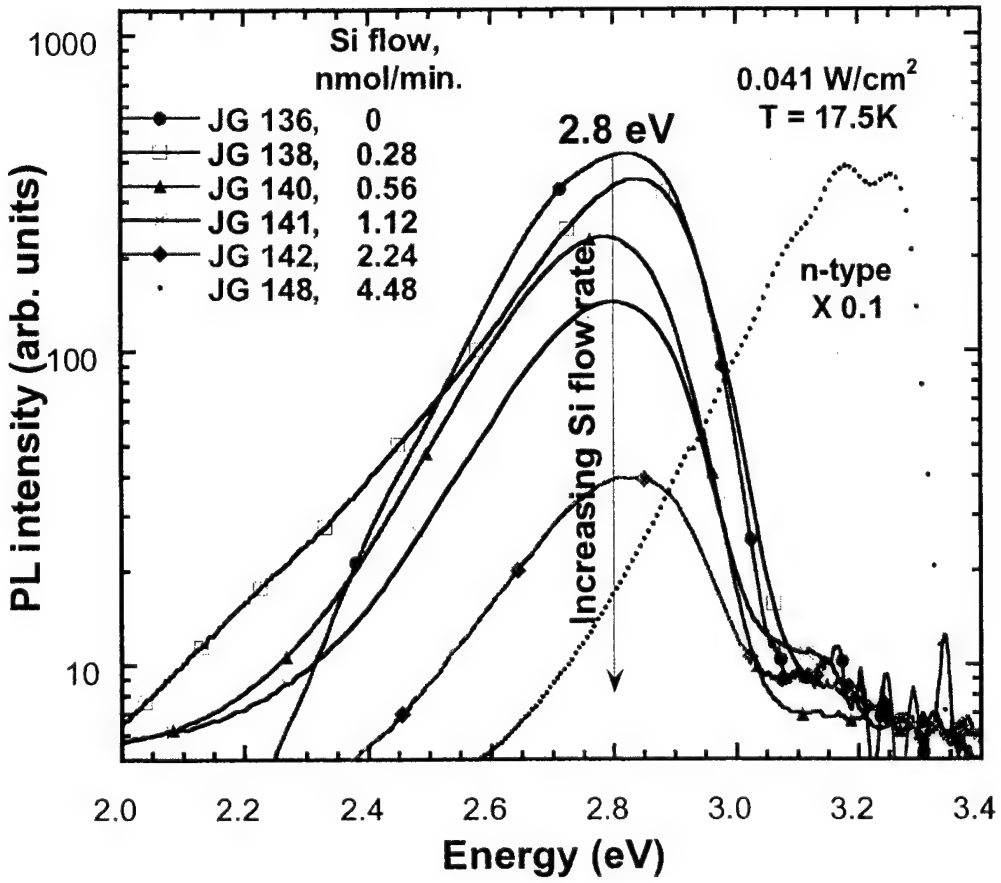
Si flow,
nmol/min.
JG 136, 0
JG 138, 0.28
JG 140, 0.56
JG 141, 1.12
JG 142, 2.24
JG 148, 4.48
2.8 eV
0.041 W/cm2
T = 17.5K
n-type
X 0.1
Increasing Si flow rate
PL intensity (arb. units)
1000
100
10
2.0
2.2
2.4
2.6
2.8
3.0
3.2
3.4
Energy (eV)

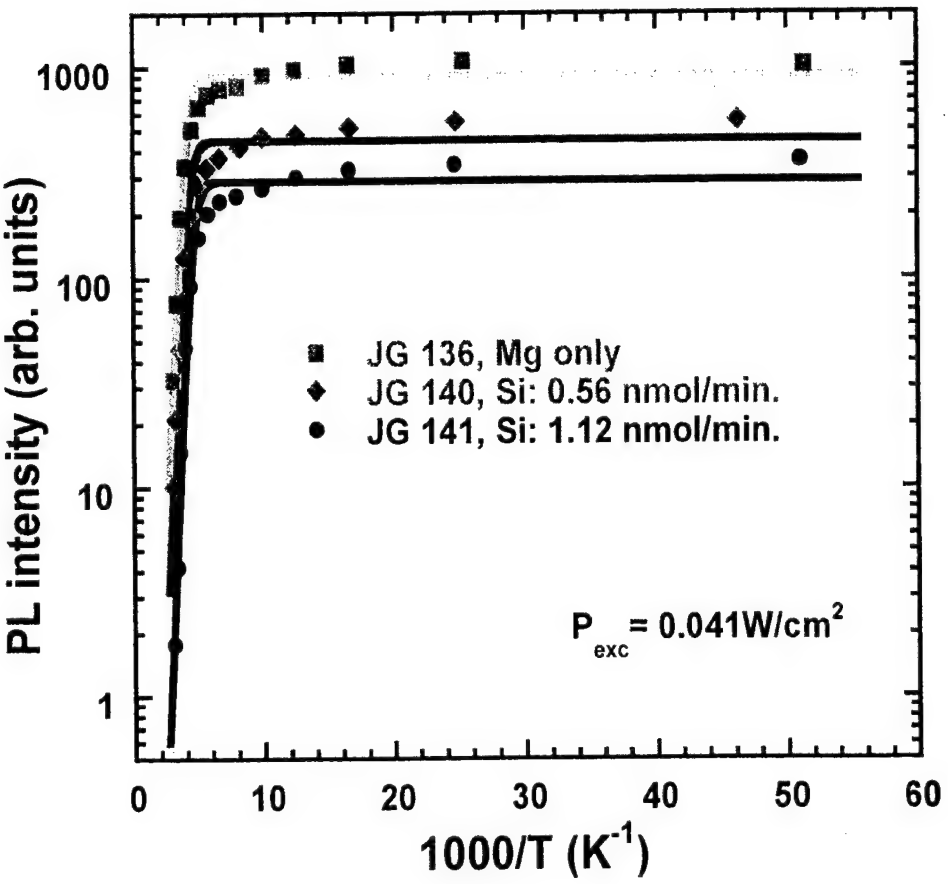
1000
100
10
1
PL intensity (arb. units)
0
10
20
30
40
50
60
1000/T (K^{-1})
JG 136, Mg only
JG 140, Si: 0.56 nmol/min.
JG 141, Si: 1.12 nmol/min.
P_{exc} = 0.041W/cm^2

Fig. 2

Fig. 3

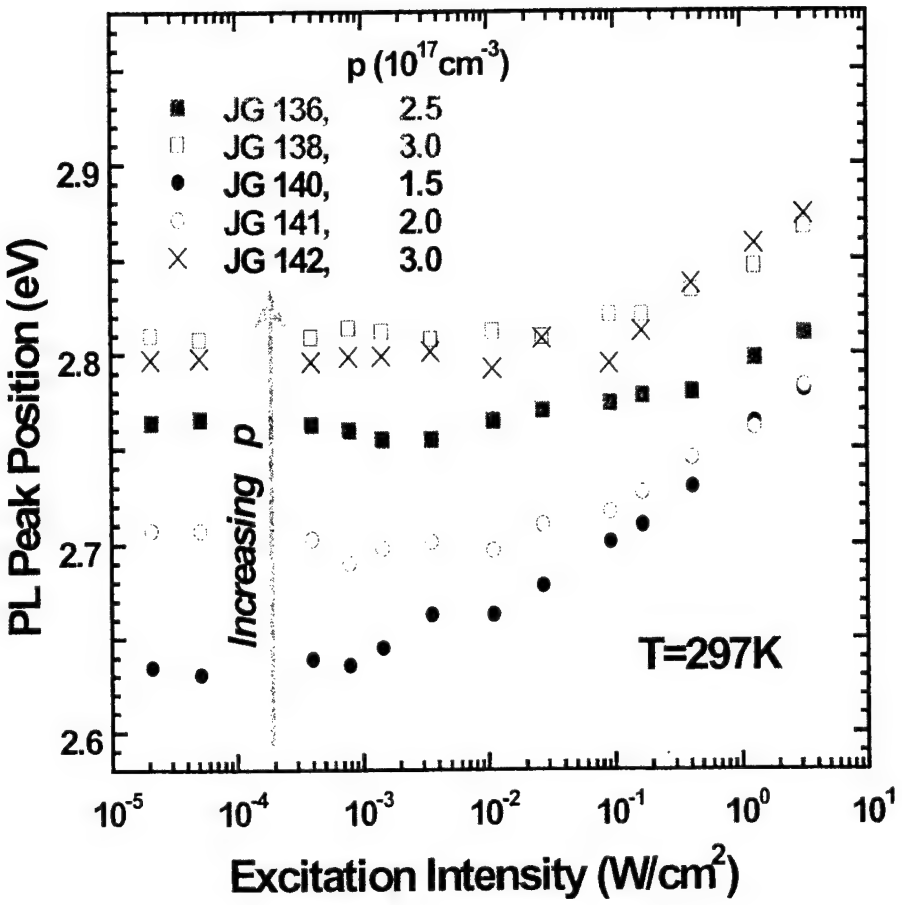
p (10^17 cm^-3)
JG 136, 2.5
JG 138, 3.0
JG 140, 1.5
JG 141, 2.0
JG 142, 3.0
Increasing p
T=297K
PL Peak Position (eV)
2.9
2.8
2.7
2.6
10^-5
10^-4
10^-3
10^-2
10^-1
10^0
10^1
Excitation Intensity (W/cm^2)

Fig. 4a

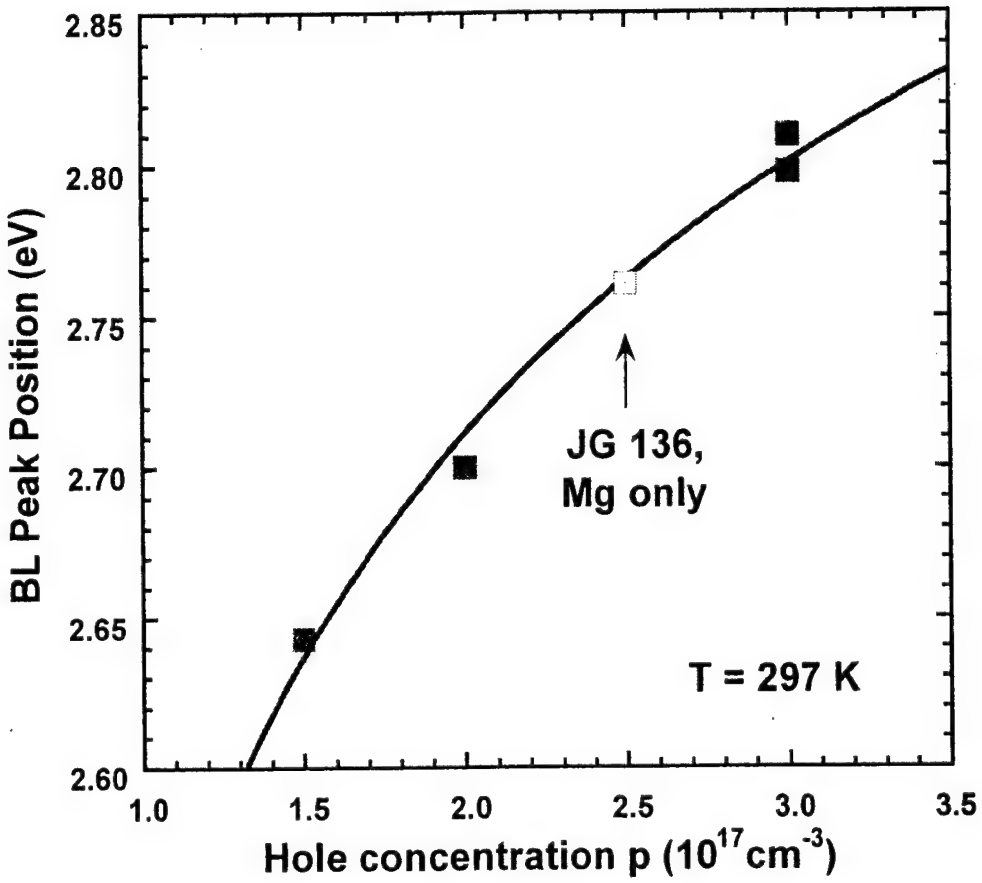
2.85
2.80
2.75
2.70
2.65
2.60
BL Peak Position (eV)
1.0
1.5
2.0
2.5
3.0
3.5
Hole concentration p (10^{17}cm^{-3})
JG 136,
Mg only
T = 297 K

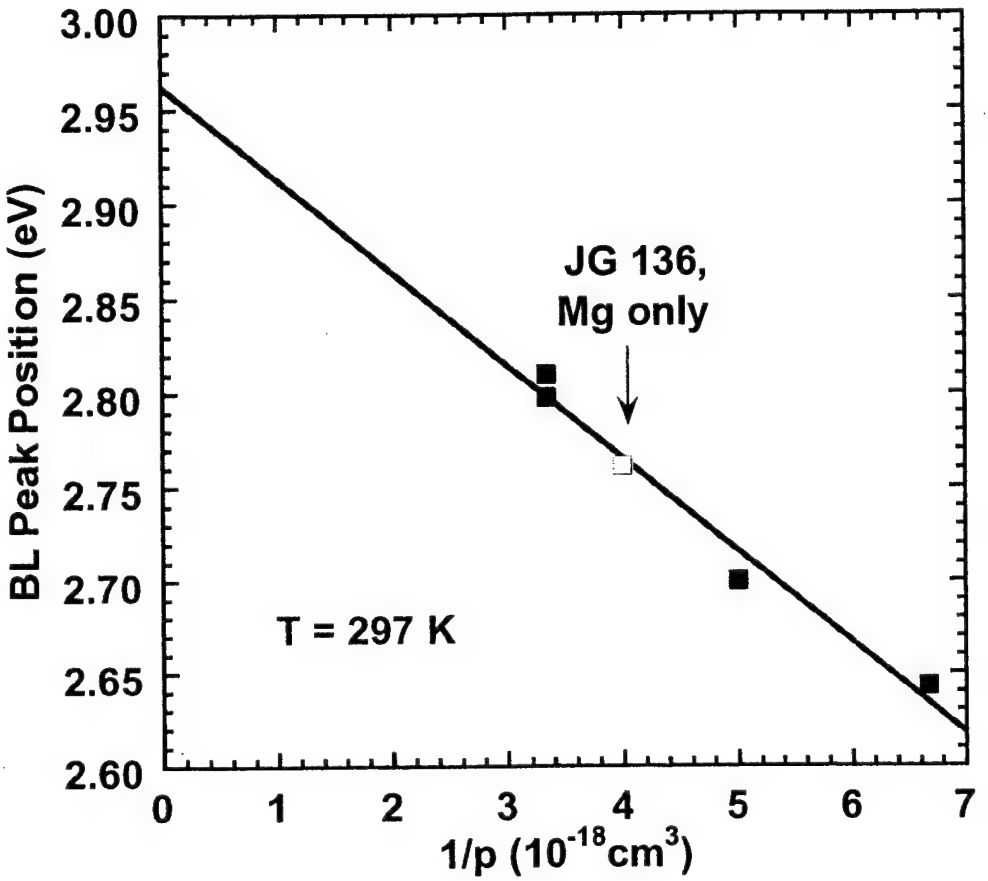
3.00
2.95
2.90
2.85
2.80
2.75
2.70
2.65
2.60
BL Peak Position (eV)
JG 136,
Mg only
T = 297 K
0
1
2
3
4
5
6
7
1/p (10^-18 cm^3)

Fig 4b

ELSEVIER

Physica B 308–310 (2001) 18–21

PHYSICA B

www.elsevier.com/locate/physb

Optical study of GaN : Mn co-doped with Mg grown by metal organic vapor phase epitaxy

R.Y. Korotkov, J.M. Gregie, B. Han, B.W. Wessels*

Department of Materials Science and Engineering, Northwestern University, Materials and Life Science Building, 2225 N. Campus Drive, Evanston, IL 60208-3108, USA

Abstract

Optical properties of a series of semi-insulating Mn-doped GaN co-doped with Mg were studied using photoluminescence (PL). A strong PL emission band at 1.0 eV was observed upon co-doping. The new band exhibited a rich fine structure with peaks at 1.057, 1.048, 1.035, 1.032, 1.020, 1.014, 1.008, 1.000 and 0.988 ± 0.001 eV. The integrated and relative intensities of these lines varied as a function of the Mn concentration and excitation source. The measured luminescence decay time was 20–95 μs and depended on emission energy.

Keywords: GaN; Photoluminescence; Mn doping

1. Introduction

The luminescence properties of the transition metal element Mn have been widely studied in III–V semiconductor compounds [1–3]. Manganese preferentially incorporates on the metal site forming an acceptor. Photoluminescence (PL) studies have shown that Mn can form donor–acceptor pairs (DAP) in these compounds. Furthermore, manganese has been shown to have intra-atomic transitions involving the d-shell electrons. The identification of the specific transition involved in optical spectra is often complicated by the presence of the two types of transitions [3,4]. Substitutional Mn will form the Mn^{2+} (d^5) and Mn^{3+} (d^4) states if placed on the cation site in III–V compounds [1–4]. It has been shown that three defect centers are formed in III–V semiconductors. They are a neutral acceptor, A^0 (d^4), an ionized acceptor (when an electron is captured by the A^0 from the valence band (VB)), A^- (d^5) and a neutral acceptor formed by a complex with a hole, A^0 (d^5+h) [5]. A negative acceptor (A^-) and complex (d^5+h) were observed for the GaAs : Mn, whereas the A^0 and A^- states were detected in GaP [5]. In GaN, the d^5 ion configuration was observed in EPR studies of unintentionally doped [6] and intentionally Mn-doped GaN [7,8].

Little is known about the Mn-related optical emission and absorption GaN. It is expected that the spin forbidden transition within Mn d^5 ion will have low intensity and long lifetime. We have recently investigated the absorption and PL spectra of Mn-doped epitaxial GaN [9]. A weak broad band was observed at 1.25 ± 0.02 eV in the PL spectra of Mn-doped samples with the full-width at half-maximum (FWHM) of 250–300 meV for above band gap excitation. The independence of the energy peak position of this band with temperature and a long ~8 ms decay times indicated that it was likely related to the spin forbidden transition, $^4T_1$–$^6A_1$ of Mn (d^5) ion [10]. The energy position for this band was similar to that (1.3 eV) for $^4T_1$–$^6A_1$ recombination observed for Fe^{3+} in GaN [11].

In this paper, PL properties of the GaN : Mn co-doped with Mg are investigated. A new strong PL band with a rich structure is observed on the low energy side of the 1.25 eV band previously reported in Mn-doped GaN samples [9].

2. Experimental

The MOVPE growth of the Mn-doped GaN layers has been previously described [9]. For the Mn, Mg co-

*Corresponding author. Tel.: +1-847491-3537; fax: +1-847-491-7820.

E-mail address: b-wessels@nwu.edu (B.W. Wessels).

0921-4526/01/$ - see front matter
PII: S0921-4526(01)00654-8

doping experiments, the Mg source partial pressure was 0.18 μmol/min[1] and Mn source partial pressure was varied in the broad range from 0.02 to 5 μmol/min. The epitaxial layer consisted of a 20 nm GaN nucleation layer, a 500 nm Mg-doped (0.03 μmol/min) layer grown at 1060°C, and a 2–2.5 μm thick Mn, Mg co-doped layer grown at 1060°C. As-grown Mn–Mg epilayers had semi-insulating behavior. The Mg co-doped samples were annealed at 850°C to produce p-type material. Photoluminescence spectra were measured over the spectral range of 0.7–1.2 eV. Photoluminescence was excited with either the 325 nm line of a He–Cd laser or a semiconductor laser with excitation wavelength of 973.8 nm. The excitation densities of these lasers were 0.32 and 3 W/cm^2, respectively. The PL signal was dispersed by a Zeiss monochromator with a resolution of 2 meV at 1 μm and detected with a high sensitivity Ge-detector and a lock-in amplifier. The sample temperature was varied from 20 to 300 K using a closed cycle helium cryostat. The He–Cd laser intensity was varied using neutral density filters in the range of 2×10^{-3}–10 W/cm^2. All PL spectra were normalized to account for the spectral responsivity of the Ge-detector as well as the monochromator. Transient PL decay curves were excited using 500 MHz pulsed 974 nm laser. The system resolution was limited by the Ge-detector rise time of 16 μs.

3. Results and discussion

A new strong band with a peak at approximately 1.0 eV was observed in the PL upon co-doping with Mg. It was composed of a series of sharp lines with FWHM of ~3–10 meV. A PL spectrum of this fine structure obtained with below band gap excitation (974 nm) is shown in Fig. 1. Note, however, that the 1.25 eV PL band observed in Mn-doped samples was not detectable above the excitation 974 nm laser noise suggesting that the new sharp emission was activated in GaN : Mn by co-doping with Mg.[2] The major energies of the sharp lines observed in the co-doped samples spectra are summarized in Table 1. They are at 1.057, 1.048, 1.035, 1.032, 1.020, 1.014, 1.008, 1.000 and 0.988 ± 0.001 eV. A few weak transitions were also observed on the lower energy side of the main band as seen in Fig. 1. This fine structure was observed with both extrinsic and intrinsic

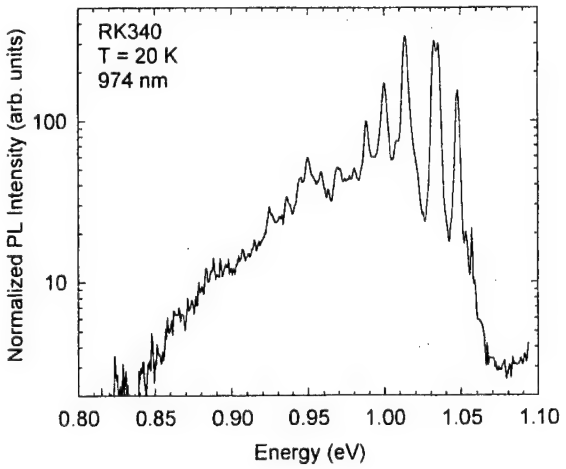

Fig. 1. PL spectrum for one of the co-doped samples (RK 340) obtained with 974 nm excitation at 20 K. The energies of the fine structure are listed in Table 1 for the strongest lines.

excitation sources [12]. It was observed with above band gap energies of 325 nm He–Cd laser as well as below band gap 632.8 and 974 nm lasers. The positions of the peaks were the same for these excitation sources. However, the integrated and relative intensities varied as a function of the excitation wavelength indicating that each major separate emission line is likely to have its own excitation spectra.

To study the effect of Mn concentration on the integrated intensity of the 1.0 eV band, a series of co-doped films were grown with different Mn concentrations. In this experiment, the Mg acceptor concentration was constant, whereas the Mn concentration varied. The normalized PL spectra for this series of samples are shown in Fig. 2. The integrated intensity of the 1.0 eV band increased at first with the increase of Mn-partial pressure and then decreased [12]. Note that the energy positions of the sharp emission lines were the same for these samples indicating that the optically active centers involved were of the same nature in all studied samples. However, relative intensities of these lines varied as a function of the Mn concentration indicating that the concentration of the optically active centers involved in the separate sharp lines changed with Mn concentration.

To detail the nature of the 1.0 eV band it was studied as a function of temperature and excitation intensity. Thermal quenching of the luminescence was studied under 974 nm excitation. All bands except one were thermally quenched above 100 K with activation energy of ~70 meV as shown in Fig. 3.[3] The intensity of the

[1] This Mg partial pressure was used to achieve $p = 2 \times 10^{17}$ cm^{-3} in Mn-doped GaN [13].

[2] It is important to note that our undoped GaN samples did not exhibit emission bands in the near infra-red. Previously observed Co^{2+}, (Cr^{4+}/Ti^{2+}) and Fe^{3+} emission bands at 1.047, 1.19 and 1.3 eV [1,14] were not detected in our undoped GaN samples. Therefore, the observed fine structure is specifically related to the Mn–Mg co-doped samples.

[3] A slightly different activation energy of 0.1 eV was calculated for the experimental data obtained under 325 nm excitation.

Table 1
Energy positions and lifetimes of sharp peaks observed in Mg co-doped GaN:Mn samples and Mn-doped samples (1.25 eV band)

Energy (eV)	1.057	1.048	1.034	1.032	1.02	1.013	0.988	0.986	0.95	1.25
τ (μs)	40	95	68	68	52	42	54	54	49	8000

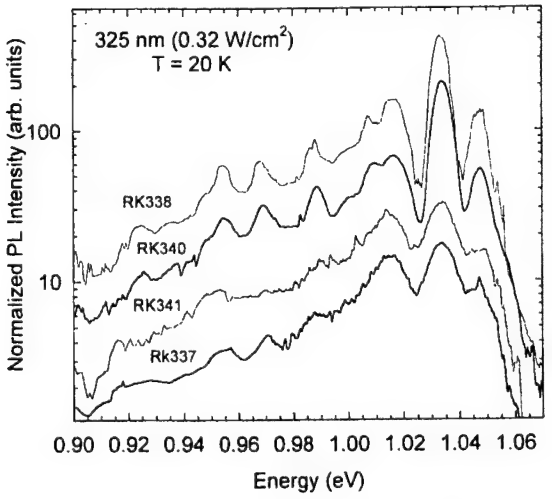

Fig. 2. Above band gap excited (325 nm) PL spectra of co-doped samples at 20 K grown with different Mn concentrations. The Mg partial pressure was constant (0.18 μmol/min). The Mn partial pressures were 4.54, 1.36, 0.079 and 0.02 μmol/min for samples RK 341, RK 340, RK 338 and RK 337, respectively.

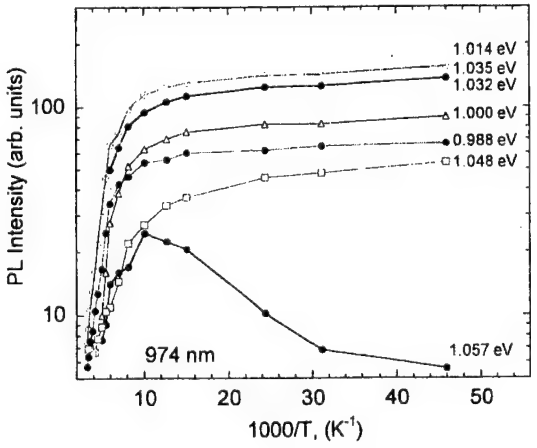

Fig. 3. Thermal quenching of the individual transitions of the 1.0 eV band excited with 974 nm excitation.

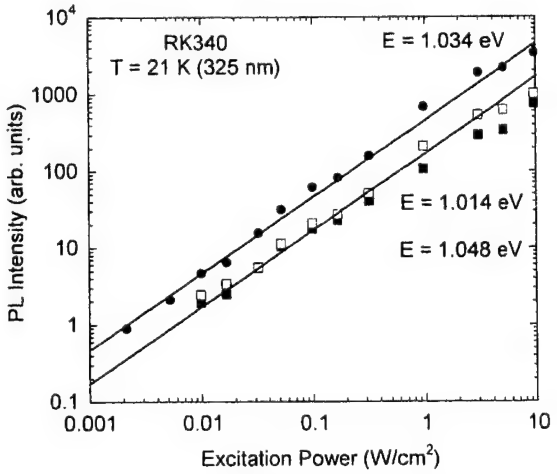

Fig. 4. Excitation intensity dependence of the PL intensity for three sharp lines obtained with above band gap excitation (325 nm) at 20 K.

highest energy transition observed at 1.057 eV first increased from 20 to 100 K and then decreased with the increase of the temperature, $T > 100$ K. The increase of 1.057 eV band was likely due to interactions with phonons. The PL intensity of the lines comprising the 1.0 eV band increased linearly with excitation power as shown in Fig. 4 for selected transitions under 325 nm excitation. In addition, for below band gap excitation the intensity of the sharp structure linearly increased with excitation power [12].

To determine whether these emission lines were associated with intra-d shell transitions, the luminescent recombination lifetime was measured on the co-doped samples. A PL decay curve for transitions at 1.032 eV is shown in Fig. 5. The PL intensity decayed exponentially at low temperature (20 K). The decay time was 66 μs. The lifetime of the sharp lines (40–90 μs) in the co-doped samples was two orders of magnitude smaller than that observed for the characteristic 1.25 eV Mn band for the Mn-doped GaN samples [10]. In this case, the lifetime was of the order of ~8 ms. Furthermore, each emission line had slightly different recombination lifetime, as shown in Table 1, suggesting that emission lines in the fine structure are associated with different recombination centers.

The dramatic change in the luminescence spectra of Mn doped GaN upon co-doping with Mg was unexpected. Its origin is not understood. Co-doping with Mg acceptors may potentially lead to several changes in

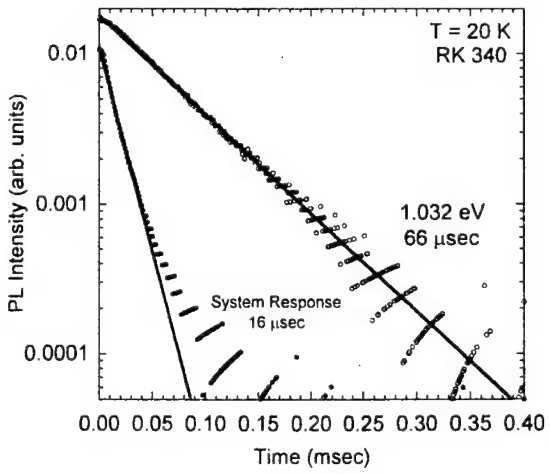

Fig. 5. Transient PL spectra of one of the co-doped samples obtained at 1.032 eV, 20 K. The calculated exponential decay (66 μs) is shown with a solid line. System response of 16 μs is shown for comparison.

the optical behavior of Mn. Addition of Mg could lead to complex formation. Furthermore, interactions with Mg may distort the Mn-ion surroundings. The alteration of the Mn-ion (d^5) surroundings changes the environmental symmetry of Mn ion leading to the breakdown of the selection rules by the appreciable sextet–quartet mixing [2,3]; consequently, the forbidden $^4T_1$–$^6A_1$ transition becomes allowed. The decrease of the lifetime for the 1.0 eV PL band by two orders of magnitude from 8 ms observed in Mn-doped GaN seems to support changes in local symmetry in co-doped samples.[4]

While co-doping with Mg could lead to changes in local symmetry, addition of Mg acceptors will also lower the Fermi energy, potentially leading to a change in the charge state of Mn. In addition, lowering of the Fermi level will result in increased compensation of the p-doped GaN with donors, D. An alternative explanation is that the observed fine structure could involve Mn^{3+}-D and Mn^{2+}-D centers. The alteration of the Fermi energy upon co-doping could potentially stabilize one of these complexes. Indeed a model involving transitions from Cr^{3+}-D to Cr^{2+}-D was proposed to explain the fine structure consisting of 19 lines observed in absorption spectrum of Cr in GaAs [4].

[4] The fact that the observed fine structure in co-doped GaN is formed on the low energy side of the 1.25 eV band in GaN:Mn can be explained by the fact that in the moderately doped GaN:Mn, two exponential decays were observed with the lifetime of 200 μs centered at 1.38 ± 0.02 eV and 8 ms centered at 1.1 ± 0.05 eV [9,14]. The last transition was assigned to $^4T_1$–$^4A_1$ recombination of Mn in GaN.

4. Conclusions

In conclusion, the luminescent properties of semi-insulating Mn-doped GaN co-doped with Mg were studied. Upon co-doping, a strong PL band at 1.0 eV was observed. The PL band displayed a rich fine structure at low temperature. It is comprised of at least 10 emission lines separated by 2–10 meV. The FWHM of these lines varied from 3 to 10 meV and was limited by the resolution of the monochromator. Transient spectroscopy measurements indicated the 1.0 eV PL band decayed exponentially with a lifetime of 20–90 μs. The measured lifetimes were at least two orders of magnitude shorter than that observed for the $^4T_1$–$^6A_1$ transition at 1.25 eV in Mn-doped GaN.

Acknowledgements

This work was supported by the Office of Naval Research under grant N00014-01-0012.

References

[1] L. Eaves, A.W. Smith, M.S. Skolnick, B. Cockayne, J. Appl. Phys. 53 (1982) 4955.
[2] L. Samuelson, M.-E. Pistol, S. Nilson, Phys. Rev. B 33 (1986) 8776.
[3] F. Bantien, J. Weber, Phys. Rev. B 37 (1988) 10111.
[4] M. Jaros, Deep Levels in Semiconductors, Adam Hilger Ltd., Bristol, 1982.
[5] J. Szczytko, A. Twardowski, K. Swiatek, M. Palczewska, M. Tanaka, T. Hayashi, K. Anado, Phys. Rev. B 60 (1999) 8304.
[6] P.G. Baranov, I.V. Ilyin, E.N. Mokov, A.D. Roenkov, Semicond. Sci. Technol. 11 (1996) 1843.
[7] W. Gebicki, J. Strzeszewski, G. Kalmer, T. Szyszko, S. Podsiadlo, Appl. Phys. Lett. 76 (2000) 3870.
[8] M. Zajac, R. Doradzinski, J. Gorsk, J. Szczytko, M. Lefeld-Sosnowska, M. Kaminska, A. Twardowski, M. Palczewska, E. Grzanka, W. Gebicki, Appl. Phys. Lett. 78 (2001) 1276.
[9] R.Y. Korotkov, J.M. Gregie, B.W. Wessels, in: U. Mishra, M. Shur, C. Wetzel, B. Gil, K. Katsumi (Eds.), GaN and Related Alloys 2000, Proc. Mat. Res. Soc. Symp. G3(7) 2000.
[10] R.Y. Korotkov, J.M. Gregie, B.W. Wessels, in these Proceedings (ICDS-21), Physica B 308–310 (2001).
[11] R. Heitz, A. Hoffman, I. Broser, Phys. Rev. B 55 (1997) 4382.
[12] R.Y. Korotkov, J.M. Gregie, B.W. Wessels, to be published.
[13] R.Y. Korotkov, J.M. Gregie, B.W. Wessels, Appl. Phys. Lett. 78 (2001) 222.
[14] K. Pressel, S. Nilsson, R. Heitz, A. Hoffmann, B.K. Meyer, J. Appl. Phys. 79 (1996) 3214.

ELSEVIER

Physica B 308–310 (2001) 30–33

PHYSICA B

www.elsevier.com/locate/physb

Mn-related absorption and PL bands in GaN grown by metal organic vapor phase epitaxy

R.Y. Korotkov, J.M. Gregie, B.W. Wessels*

Department of Materials Science and Engineering and Materials Research Center, Northwestern University, Materials and Life Science Building, 2225 N. Campus Drive, Evanston, IL 60208-3108, USA

Abstract

In this paper, the optical absorption and photoluminescence spectra of semi-insulating Mn-doped GaN films were studied. Two characteristic bands were observed in the absorption spectra of Mn-doped epilayers at 300 K. The integrated intensities of these bands increased with increasing Mn concentration indicating that they were Mn-related. An analysis of the temperature behavior of the absorption band with a maximum at 1.5 eV indicated that it involved a free to bound transition from the valence band to the deep Mn-acceptor level. Photoluminescence measurements of Mn-doped films indicated the presence of an intra 3d-shell transition of the Mn ion. The luminescence band at 1.25 ± 0.02 eV is tentatively attributed to the $^4T_1(G) \rightarrow {}^6A_1(S)$ transition.

Keywords: Gallium nitride; Transition metals; Manganese; Absorption

1. Introduction

Manganese has extensively been studied as a dopant in II–VI [1] and III–V [2,3] materials for optical applications [3]. The features of the optical spectra of Mn-doped films have usually been assigned to internal 3d-shell transitions within the Mn ion. The free Mn^{2+} ion with d^5 electron configuration has a ^6S ground and a ^4G first excited state [2]. A crystal field of trigonal symmetry in the wurtzite structure leads to the splitting of the ^4G excited state into three states, $^4T_1$, $^4T_2$ and $^4A_1$, (from the lowest to the highest energy) [4–7]. The ground state of the Mn ion, $^6A_1$, is unaffected by the crystal field. Therefore, a series of transitions including $^6A_1$–$^4T_1$, $^6A_1$–$^4T_2$ and $^6A_1$–$^4A_1$ are often observed in absorption for Mn in wide gap hosts.

Manganese has been shown to form an acceptor level when it substitutes in the group-III metal site [2]. The binding energy of the Mn acceptor varies from 113 meV in GaAs to 400 meV in GaP and InP [2,3,8]. The binding energies of Mn were found to follow a universal trend [9]. Caldas et al. indicated that the transition metal binding energies are referenced to the vacuum level and independent of the band edges of the host crystal [9].

The behavior of Mn in GaN has received limited attention [10]. However, electron paramagnetic resonance (EPR) studies of residual Mn impurities in GaN grown by the sublimation 'sandwich method' [11] and GaMnN grown by the ammonothermal method [12] unambiguously identified the presence of the Mn^{2+} d^5 ion. Furthermore, Raman scattering studies of GaMnN observed new bands around 300 and 667 cm^{-1} [12]. We previously reported our preliminary data on the absorption and PL spectra of deliberately Mn-doped GaN grown by metal organic vapor phase epitaxy (MOVPE) [13,14]. It was shown that Mn introduced two well-resolved characteristic absorption bands in the GaN thin films. In this paper, the optical properties of a series of GaN samples deliberately doped with Mn are reported.

2. Experimental

The MOVPE growth of Mn-doped GaN layers has been previously described [13]. Optical absorption–

*Corresponding author. Tel.: +1-847-491-3537; fax: +1-847-491-7820.

E-mail address: b-wessels@northwestern.edu (B.W. Wessels).

0921-4526/01/$ - see front matter
PII: S0921-4526(01)00660-3

reflection measurements at room temperature and in the 300–1200 nm range were performed using a Cary-500 spectrometer. Absorption spectra at 20–300 K were measured in the range 0.8–1.63 eV using a quartz halogen lamp and Zeiss monochromator with a resolution of 1.5 nm at 1 μm. A Ge-detector was used to measure transmittance of the sample. All absorption spectra were normalized to account for the spectral responsivity of the lamp and Ge-detector as well as the monochromator. Transient PL decay curves were excited using 20 Hz, 4 ns pulses of N_2 laser with an excitation energy of 3.68 eV. The signal was detected using a Hammamatsu photomultiplier tube (R632) with a rise time of 9 ns.

3. Results and discussion

The normalized reflectance spectra of a series of undoped and Mn-doped samples at room temperature are shown in Fig. 1. The studied samples are reported in Table 1. It can be seen from Fig. 1 that in addition to the characteristic band gap absorption at 3.4 eV, observed in the undoped sample, two new well-resolved bands have been observed for the Mn-doped samples. The first band has a minimum at 1.5 ± 0.02 eV with a full width half maximum (FWHM) of 370 meV. The second band has an onset at 2.0 eV and a minimum at 2.8 ± 0.05 eV. Its asymmetrical shape indicates that it may be comprised of two separate bands. The absolute intensities of these two bands increase systematically with an increase of the Mn dopant, indicating that they are Mn-related.

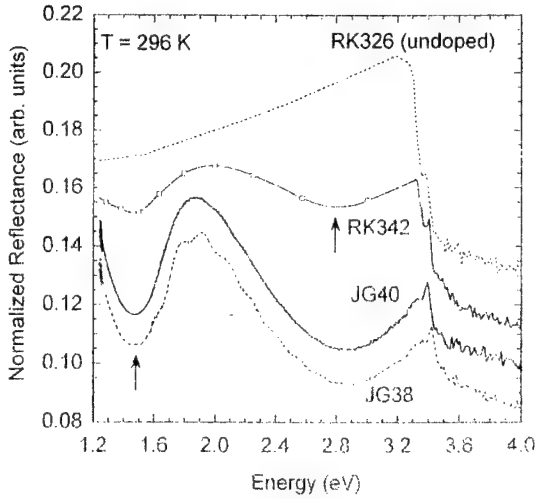

Fig. 1. Room temperature reflectance spectra of undoped, and a series of Mn-doped samples (Table 1). Two new transitions at 1.5 and 2.9 eV observed in Mn-doped samples are labeled with arrows.

Table 1
Absorption coefficients and resistivities of undoped and Mn-doped films at $T = 296$ K

Sample #	Mn (μmol/min)	Resistivity (Ω cm)	α (2.9 eV) (cm^{-1})	α (1.5 eV) (cm^{-1})
JG38	12.7	>100	3688	1405
JG40	7.6	>100	3232	1221
RK342	4.5	>100	1076	330
RK326	Undoped	0.1	—	—

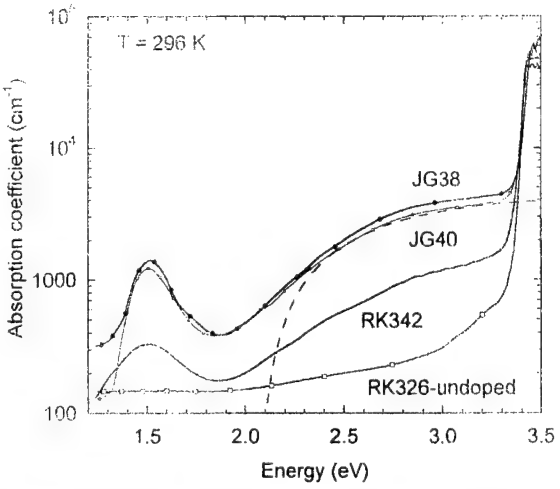

Fig. 2. Absorption coefficient as a function of energy for a series of undoped and Mn-doped samples listed in Table 1. The dashed line is a calculated fit using an ionization energy of 2.1 eV.

To determine the absorption coefficient of Mn-doped GaN films, polarized ($E\perp c$) transmission and reflection spectra were measured at 295 K. The absorption coefficient was calculated based on these measurements [13]. The dependence of the absorption coefficient as a function of energy for undoped and a series of Mn-doped epilayers is shown in Fig. 2. The maximum values of the absorption coefficient for the observed bands are also presented in Table 1. The nominally undoped GaN film is transparent in the visible region with the band edge absorption onset at $E_g\sim3.42\pm0.02$ eV at room temperature. However, two absorption bands are formed in Mn-doped GaN. The first band has an onset at 1.4 eV and a maximum at 1.5 ± 0.01 meV. This band has an asymmetrical shape with an FWHM of 245 ± 10 meV. The second band is seen as a broad shoulder with an onset at 2.1 eV. This absorption occurs over a wide energy range (2.1–2.9 eV). The intensity of both bands systematically increased with Mn dopant as shown in Table 1.

The low temperature absorption spectrum of GaN:Mn was measured. The variation of the absorption band shape with temperature for the 1.5 eV band is shown in Fig. 3. At 20 K, a fine structure was resolved. We attributed the first sharp peak at 1.418 ± 0.001 eV to the zero-phonon line (ZPL) of the Mn free to bound acceptor transition, E_0 [14]. The fine structure at higher energies of the low temperature spectrum was attributed to coupling with two local vibration modes with energies of 20 and 73 meV. The observed fine structure is a characteristic feature of an absorption band involving a deep defect level and its phonon replicas [7,15].

With increasing temperature, however, the sharp peaks involved in the Mn-absorption band become less resolved, as seen in Fig. 3. Although the line shape changes, the total absorption intensity is approximately independent of temperature, such that as the intensity of the ZPL decreases the intensities of the side bands increase [7,15]. Therefore, the 'area conservation law', that is a characteristic feature of absorption involving a deep level, governs the behavior of the absorption spectrum at higher temperatures, as seen in Fig. 3. At room temperature a broad band (FWHM = 340 meV) is observed.

Based on the configuration coordinate analysis of the temperature-dependent behavior of the 1.5 eV band, it is concluded that this band involves a deep Mn-acceptor level, and not an internal 3d-shell transition. The position of this level is placed at 1.42 eV based on the ZPL. The level position with respect to the valence band is at $E_A = E_V + 1.42$ eV based on deep level optical spectroscopy measurements [14]. The threshold of the 2.1 eV band was independent of temperature (22 and 300 K), as seen in Fig. 4. Weak shoulders were also observed in the absorbance curve at 2.3 ± 0.05 and 2.7 ± 0.05 eV at $T = 22$ K.

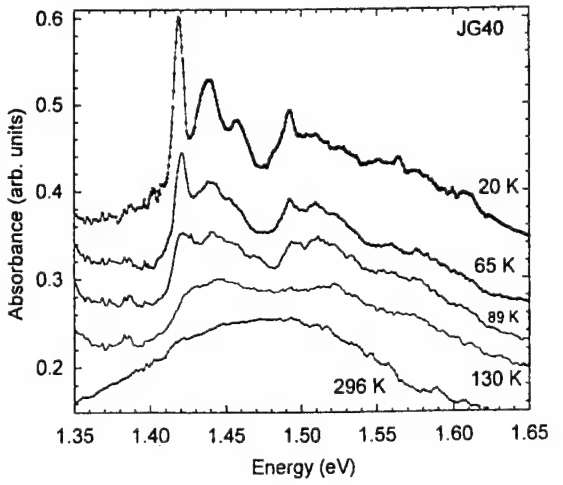

Fig. 3. Absorbance spectra of the heavily Mn-doped film at different temperatures.

A broad PL band at 1.25 ± 0.02 eV was observed in Mn-doped samples [13]. The peak position of this band was independent of temperature. The transient decay curves obtained for the 1.25 eV band at different temperatures for one of the samples are shown in Fig. 5. The decay was exponential at low temperature. The calculated decay curve ($\tau = 7.8$ ms) is shown with a solid line in Fig. 5. A long decay time is a characteristic feature of forbidden transitions, such as $^4T_1 \rightarrow {}^6A_1$ [2,6]. At high temperature, the decay time decreases and the decay curves become non-exponential. Similar behavior was observed for the Mn internal transitions in ZnS, where long decay times of 1.6 ms were measured [16]. In that case, the decay curve was non-exponential due to non-radiative recombination processes that become important at high temperatures for the Mn ion.

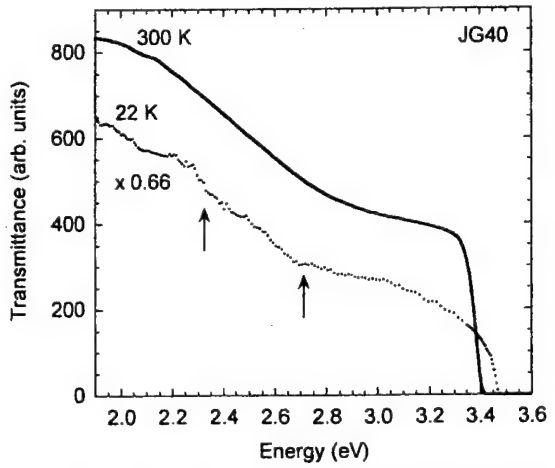

Fig. 4. Absorption spectra of the heavily Mn-doped films at 22 and 300 K.

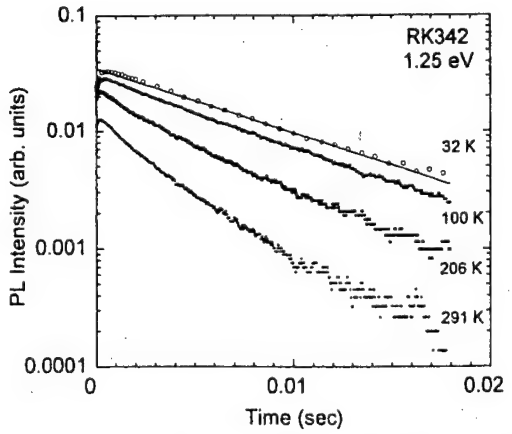

Fig. 5. PL decay curves at 1.25 eV measured at different temperatures (RK342). The calculated exponential decay with a lifetime of 7.8 ms is shown with a solid line.

A proposed energy level scheme for Mn in GaN is as follows: the Mn-acceptor level is located at $E_v + 1.42$ eV. The observed higher lying absorption bands at 2.1 and 2.8 eV are tentatively associated with electron excitation from this level to the conduction band[1] and electron excitation from the VB to the first excited state ($^4T_1$).[2,3] The observed photoluminescence band at 1.25 eV is attributed to an intra d-shell transition from the first excited state to the ground state given as $^4T_1 \rightarrow {}^6A_1$. Higher lying 3d excited states are believed to be degenerate with the conduction band and thus, are not observed in photoluminescence measurements.

4. Conclusions

The optical absorption and photoluminescence properties of semi-insulating Mn-doped GaN films were studied. Two characteristic absorption bands were observed in the spectrum of Mn-doped epilayers at 300 K. The integrated intensities of these bands increased with increasing Mn concentration, indicating that they were Mn related. An analysis of the temperature behavior of the absorption band with a maximum at 1.5 eV indicated that it involved a free to bound transition from the valence band to the deep Mn-acceptor level. Photoluminescence measurements of Mn-doped films indicated the presence of an intra 3d-shell transition of the Mn ion. The luminescence band at 1.25 ± 0.02 eV is tentatively attributed to the $^4T_1(G) \rightarrow {}^6A_1(S)$ transition.

Acknowledgements

This work is supported by the NSF GOALI program under grant DMR-9705134 and ONR grant # N00014-01-0012.

[1] This assignment assumes a large degree of compensation of the GaN, which is usually the case.

[2] The higher lying intra-ion transitions, $^6A_1 \rightarrow {}^4T_2$ and $^6A_1 \rightarrow {}^4A_1$ are likely to occur at 2.1 and 2.7 eV based on the observed transition in GaN:Fe^{3+} [5] absorption spectra, however, the intensity of these forbidden transitions has to be small. In contrast, large absorption coefficients were measured for the 2.1 eV band (Table 1), which were higher than that of the 1.5 eV band.

[3] It is important to note, however, that several different states of Mn, such as Mn^{2+}, Mn^{3+}, Mn^{4+} can potentially introduce several deep levels in the band gap giving rise to several free to bound transitions as in Ref. [7].

References

[1] W. Park, T.C. Jones, W. Tong, S. Schon, M. Chaichimansour, B.K. Wagner, J. Appl. Phys. 84 (1998) 6852.
[2] F. Bantien, J. Weber, Phys. Rev. B 37 (1988) 10111.
[3] V.F. Masterov, B.E. Samorukov, Sov. Phys. Semicond. 12 (1977) 363.
[4] R. Heitz, A. Hoffmann, I. Broser, Phys. Rev. B 45 (1992) 8977.
[5] R. Heitz, A. Hoffmann, I. Broser, Phys. Rev. B 55 (1997) 4382.
[6] D.S. McClure, Solid State Phys. 9 (1954) 488.
[7] B. Henderson, G.F. Imbusch, Optical Spectroscopy of Inorganic Solids, OUP, Oxford, 1989.
[8] S.A. Abagyan, G.A. Ivanov, G.A. Koroleva, Y.N. Kuznetsov, Y.A. Okunev, Sov. Phys. Semicond. 9 (1975) 243.
[9] M.J. Caldas, A. Fazzio, A. Zunger, Appl. Phys Lett. 45 (1984) 671.
[10] P.G. Baranov, I.V. Ilyin, E.N. Mokov, A.D. Roenkov, Semicond. Sci. Technol. 11 (1996) 1843.
[11] M. Zajac, R. Doradzinski, J. Gorsk, J. Szczytko, M. Lefeld-Sosnowska, M. Kaminska, A. Twardowski, M. Palczewska, E. Grzanka, W. Gebicki, Appl. Phys. Lett. 78 (2001) 1276.
[12] W. Gebicki, J. Strzeszewski, G. Kamer, T. Szyszko, S. Podsiadlo, Appl. Phys. Lett 76 (2000) 3870.
[13] R.Y. Korotkov, J.M. Gregie, B.W. Wessels, in: U. Mishra, M. Shur, C. Wetzel, B. Gil, K. Katsumi (Eds.), GaN and Related Alloys 2000, Proc. Mat. Res. Soc. Symp. G3.7 (2000).
[14] R.Y. Korotkov, J.M. Gregie, B.W. Wessels, unpublished.
[15] K.K. Rebane, Impurity Spectra of Solids, Plenum, New York, 1970.
[16] W. Park, T.C. Jones, S. Schon, W. Tong, M. Chaichimansor, B.K. Wagner, C.J. Summers, J. Cryst. Growth 184–185 (1998) 1123.

Optical properties of the deep Mn acceptor in GaN:Mn

R. Y. Korotkov, J. M. Gregie, and B. W. Wessels[a)]
Department of Materials Science and Engineering and Materials Research Center, Northwestern University, Evanston, Illinois 60208

(Received 20 August 2001; accepted for publication 30 December 2001)

The optical and electrical properties of Mn-doped epitaxial GaN were studied. Low-temperature optical absorption measurements indicate the presence of a Mn-related band with a well-resolved fine structure. The zero-phonon line is at 1.418±0.002 eV with a full width at half maximum of 20±1 meV. Two pseudolocal vibrational modes associated with manganese were observed with energies of $h\nu_1$=20 and $h\nu_2$=73 meV. Deep-level optical spectroscopy measurements on lightly Mn-doped samples indicate that Mn forms a deep acceptor level at E_v+1.42 eV. Using the vacuum referred binding energy model for transition metals and the measured Mn energy level, the electron affinity of GaN is calculated to be 3.4 eV, which agrees well with experimental values. © *2002 American Institute of Physics.* [DOI: 10.1063/1.1456544]

While the optical properties of shallow impurities in GaN have been widely studied, the behavior of deep-level defects in this material is not well established. This is especially the case for transition metals. The open *d*-shell configuration of transition metals often results in the formation of localized deep levels in the band gap that are characteristic of the impurity.[1,2] Since these metals introduce deep levels, they can be used as dopants to obtain semi-insulating material in III–V semiconductors.[3] Recently, there also has been interest in transition-metal dopants to enable formation of ferromagnetic semiconductors. Of particular interest is manganese, which has been shown to form a ferromagnetic semiconductor alloy with InAs and GaAs.[4] However, little is known about its behavior in GaN.[5,6] Previously, electron paramagnetic resonance (EPR) studies unambiguously identified the presence of the Mn^{2+} ion in GaN bulk crystals from its hyperfine structure due to interactions of ^{55}Mn (I=5/2) nuclei.[1] EPR measurements of microcrystalline $Ga_{1-x}Mn_xN$ were also performed on samples with a Mn content of x=0.005 prepared by the ammonothermal method.[5] Electron spin resonance measurements indicated the presence of the Mn^{2+} (d^5) ion, and paramagnetic behavior was observed. The absorption and photoluminescence (PL) of Mn-doped GaN layers obtained by metal–organic vapor-phase epitaxy (MOVPE) were recently studied.[6] Two characteristic absorption bands were reported in the absorption spectra of Mn-doped epilayers at 296 K.[6] The high-energy absorption band had a threshold at 2.1 eV and was very broad. The low-energy band had a threshold at 1.4 eV with a maximum at 1.5±0.02 eV, and a full width half maximum (FWHM) of 245±10 meV at 296 K. This band was tentatively attributed to a free-to-bound transition involving a deep Mn acceptor level.[6] Hall-effect measurements supported this conclusion, since as-grown as well as nitrogen annealed GaN:Mn films were semi-insulating with ρ>100 Ω cm, whereas undoped crystals were typically *n* type and conducting.[7]

In order to establish the ionization energy and the energy-level positions with respect to the band edge, detailed optical measurements are required. In this letter, low-temperature absorption spectra were measured to determine the optical ionization energy of Mn in GaN. The absorption measurements indicate that Mn forms a deep acceptor level at 1.42 eV. From deep-level optical spectroscopy (DLOS) measurements, it is concluded that the optical ionization energy is with respect to the valence band.

The Mn-doped samples used in this study were grown by MOVPE as previously described.[6] The epitaxial layer consisted of a 20 nm GaN nucleation layer, a 500 nm undoped GaN layer grown at 1060 °C, followed by a 2–2.5-μm-thick Mn-doped layer also grown at 1060 °C. Absorption spectra at low temperature were measured in the energy range of 0.8–1.63 eV with a 250 W quartz–halogen lamp and a Zeiss MM12 double-prism monochromator with resolution of 1.5 nm at 1 μm. A Ge detector was used to measure the sample transmittance. The absorption spectra were normalized to account for the spectral responsivity of the lamp, monochromator, and detector. The sample temperature was varied from 20 to 300 K using a closed-cycle helium cryostat.

DLOS measurements[8] were performed on lightly Mn-doped Schottky diodes, which were *n* type. To fabricate the diodes, Au dots with a diameter of 475 μm were deposited through a shadow mask using e-beam evaporation. Indium was used as the Ohmic contact. Measurements were taken over the spectral range of 0.80–3.45 eV, at 0.05 eV intervals. Monochromatic light was provided by the same lamp and monochromator setup used for the absorption measurements. The diodes were cooled to 78 K with a liquid-nitrogen cryostat to minimize any thermal ionization effects. To record an individual scan, the sample was first forward biased in the dark to 1 V for 10 s to partially fill the traps. Next, the diode was reverse biased in the dark to −1 V and allowed to stabilize for 20 s. Subsequently, the shutter was opened and the optical emission at a specific wavelength was recorded for 1 min with a Boonton 72B capacitance meter operating at 1 MHz. For DLOS measurements, the derivative of the transient response at each wavelength was determined over the time interval of approximately 10–20 s, and was normalized to the excitation intensity.

Figure 1 shows the optical absorption of Mn-doped GaN

a)Electronic mail: b-wessels@nwu.edu

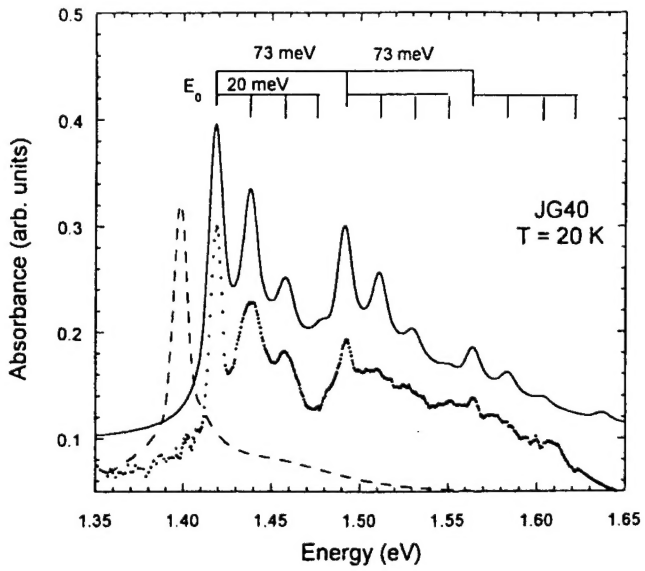

FIG. 1. Low-temperature (20 K) absorbance spectrum of highly Mn-doped GaN is shown with a dotted line. The ZPL, E_0 is at 1.418 eV. Two sets of sharp peaks with energy separations of 20 and 73 meV are seen. The calculated absorbance spectrum using Eq. (1) with Huang–Rhys factors of $S_1=1.1$ and $S_2=0.9$ is shown with a solid line. The single peak (dashed line) on the left side of the ZPL is the simulated shape of the ZPL.

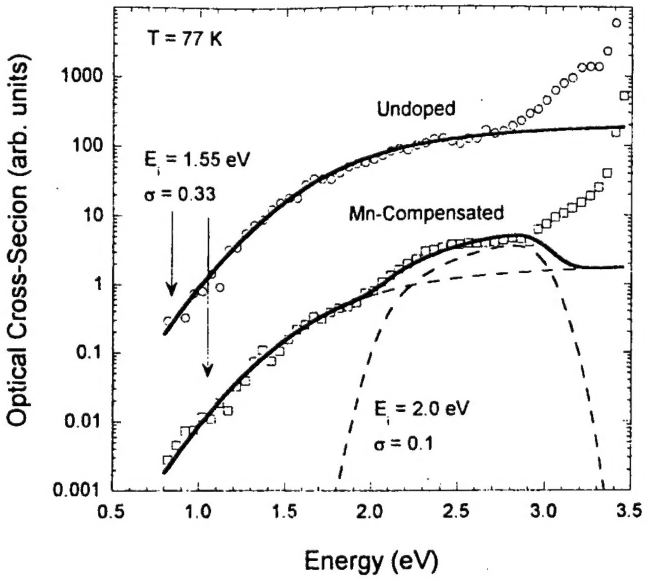

FIG. 2. Optical cross sections as a function of energy at 77 K of Mn-doped and undoped n-type samples. The calculated dependence of the cross section using Eq. (2) with $E_i=1.55$, $\sigma=0.33$ for the undoped sample is shown with a solid line. An additional peak with $E_i=2.0$, $\sigma=0.1$ was observed for the Mn-compensated sample (dashed line). The sum of the peaks in the Mn-doped sample is shown with a solid line.

at low temperataure, using polarized light ($E\perp c$). A band consisting of a series of sharp peaks is observed. The lowest-energy peak at 1.418 ± 0.002 eV is attributed to a zero-phonon-line (ZPL) transition. An analysis of the spectra indicates that the fine structure is formed by superposition of two series of peaks. The distance between peaks in the first set is $h\upsilon_1=20\pm1$ meV. This set is repeated at energies of $h\upsilon_2=73$ meV.

Observation of fine structure in absorption spectra enables determination of the vibrational characteristics of the defect in the excited state. The ZPL at 1.418 ± 0.002 meV eV has a FWHM of 20 meV. Its replicas at energy multiples of 20 ± 1 meV are attributed to transitions involving pseudolocal vibrational modes of the Mn acceptor. Repetition of this set over 73 meV demonstrates coupling with another pseudolocal vibration mode with higher energy. The frequency of the pseudolocal modes of Mn can be estimated using the simple mass defect approximation.[9–11] The calculated values are 19.7 and 72.7 meV, which is in excellent agreement with the experimental values. Therefore, the Mn acceptor forms a deep defect that is coupled with two pseudolocal vibrational modes in GaN.

In the case of two vibrational modes, the intensity of the phonon replica corresponding to emission of m and n pseudolocal phonons, W_{mn} is given by[12]

$$W_{mn}\propto\frac{S_1^m S_2^n}{m!n!}, \tag{1}$$

where S_1 and S_2 are the Huang–Rhys factors describing the coupling with two pseudolocal vibrational modes. Equation (1) was used to calculate the shape of the absorption band. The calculated absorption band obtained using Eq. (1) with $S_1=1.1$ (for the pseudolocal phonons with $h\upsilon_1=20$ meV) and $S_2=0.9$ (for the pseudo local phonons with $h\upsilon_2=73$ meV) is shown in Fig. 1 by the solid curve. It was assumed for simplicity that the shape of the phonon replicas is identical to that of the zero-phonon line, which in turn was simulated (dashed line on the left side of the absorption spectra in Fig. 1). It can be seen from Fig. 1, that a good quantitative fit was obtained using Eq. (1).[12–15]

With increasing temperature the sharp peaks of the Mn-absorption band broaden.[16] The intensity of the ZPL also decreases with temperature. However, the total integrated intensity of the absorption band remains approximately constant such that at room temperature an asymmetric broad absorption band (FWHM=340 meV) is observed.[6]

To determine the position of the deep Mn acceptor level with respect to the band edge, DLOS was used. DLOS measurements were performed on n-type GaN that was lightly doped with Mn. The electron concentration of this sample was 2×10^{16} cm^{-3} at 300 K. The DLOS spectra of Mn-compensated samples are shown in Fig. 2. In the Mn-compensated sample a new deep-level transition with a threshold at approximately 2.0 eV was observed. For comparison, it can be seen from Fig. 2 that three additional deep-level transitions are observed in both the Mn-doped and the unintentionally doped GaN sample at approximately 1.5, 2.9, and 3.3 eV, which are not Mn related.

To calculate the ionization energy of the Mn deep level, the method of Mooney *et al.*[17] is employed.[18] In this model, the photoionization cross section is convoluted with a Gaussian broadening function. There are two adjustable parameters, optical ionization energy E_i and broadening term σ. Optical cross section σ° as a function of $h\upsilon$ is given by

$$\sigma^\circ\propto\left[\frac{\sigma^{3/2}}{(h\upsilon)^2}\right]\int_0^\infty dx x^{3/2}\exp\left[-\frac{\{x-[(h\upsilon-E_i)/\sigma]\}^2}{2}\right]. \tag{2}$$

The position of the Mn-acceptor level, E_A with respect to the band edge, may be estimated on the basis of the DLOS measurements. Since an increase in capacitance was ob-

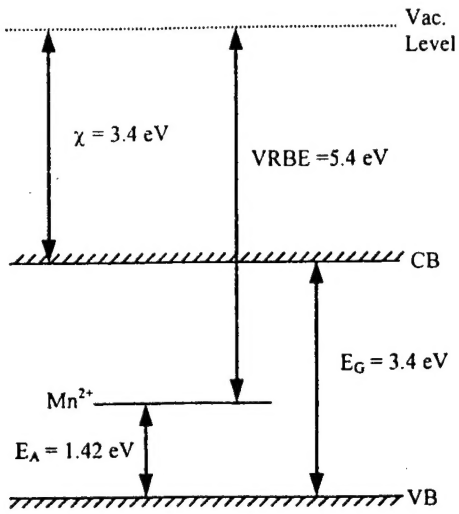

FIG. 3. Schematic energy diagram for the deep Mn acceptor in GaN.

served at 2.0 eV in an n-type sample, the transition involves electron emission from a deep acceptor to the conduction band. Therefore, the acceptor ionization energy with respect to the valence band is $E_A=E_g-E_i=3.5-2.0=1.5\pm0.1$. Note that the band gap (E_g) at 77 K is estimated as ~3.5 eV.[7] From the DLOS measurements it is concluded that the absorption band with ZPL at 1.418 eV involves a transition from the valence band into the deep Mn-acceptor level at $E_V+E_A=1.42$ eV.

The broadening term, σ, from the fit of the optical cross section obtained from the DLOS measurements gives an indication of the degree of the lattice coupling of the defect.[17] For the Mn-related peak at 2.0 eV, $\sigma=0.1$, while for the defect at 1.55 eV found in both the undoped and Mn-doped sample, $\sigma=0.33$, as shown in Fig. 2. The observed broadening supports the absorption data that indicate that the Mn acceptor is not strongly coupled to the lattice.

From the measured position of the Mn acceptor, the value of the electron affinity of GaN can be obtained using the vacuum referred binding energy (VRBE) model, which predicts the position of the transition metal with respect to the vacuum level.[3] In this model electron affinity χ is equal to $\chi=E_{\mathrm{VRBE}}+E_A-E_g$, where E_A is the Mn ionization energy obtained from experiment and E_{VRBE} is the vacuum referred binding energy. If we assume that the Mn present in our samples is in the Mn^{2+} state, the calculated E_{VRBE} is 5.4 eV.[3] Therefore, calculated electron affinity χ of GaN is 3.4 ±0.1 eV for $E_g=3.4$ eV (Ref. 7) and $E_A=1.4\pm0.1$ eV for GaN at 300 K. For comparison using ultraviolet photoemission spectroscopy, the measured electron affinity of GaN has been reported to be 3.2 ± 0.2,[19] 3.5 ± 0.1,[20] and 4.1 ± 0.1 eV.[21] Note that Pankove and Schade[21] in their letter indicated that the 4.1 eV value is the upper limit of the electron affinity of GaN. Therefore, the calculated electron affinity of 3.4 eV for GaN obtained from the VRBE model and the measured manganese energy-level position agrees well with the experimentally measured values.[19,20] This finding supports the conclusion that Mn forms an acceptor level in the band gap of GaN that is predicted by VRBE theory.[22,23] It also agrees with recent local density functional calculations of Mn in GaN, where it was predicted that the Mn level sits 1.44 eV above the valence-band maximum.[24] The band diagram indicating the position of Mn is shown in Fig. 3.

In summary, the low-temperature optical properties of Mn centers in GaN have been measured by optical absorption. Mn is a deep level in GaN. The optical ionization energy is 1.418 eV as determined from the zero-phonon-line position. From DLOS measurements the Mn level is located at $E_v+1.4$ eV. The measured position is in good agreement with theoretical predictions based on the VRBE model and experimental electron affinity values of GaN.

The authors would like to acknowledge the valuable discussion with Dr. M. A. Reshchikov and Dr. V. Litvinov. This work is supported by ONR Grant No. N00014-01-0012.

[1] P. G. Baranov, I. V. Ilyin, E. N. Mokov, and A. D. Roenkov, Semicond. Sci. Technol. **11**, 1843 (1996).
[2] D. S. McClure, Solid State Phys. **9**, 488 (1954).
[3] M. J. Caldas, A. Fazzio, and A. Zunger, Appl. Phys. Lett. **45**, 671 (1984).
[4] H. Ohno, Science **281**, 951 (1998)
[5] M. Zajac, R. Doradzinski, J. Gorsk, J. Szczytko, M. Lefeld-Sosnowska, M. Kaminska, A. Twardowski, M. Palczewska, E. Grzanka, and W. Gebicki, Appl. Phys. Lett. **78**, 1276 (2001).
[6] R. Y. Korotkov, J. M. Gregie, and B. W. Wessels, Mater. Res. Soc. Symp. Proc. **639**, G3.7 (2000).
[7] M. A. Reshchikov, F. Shahedipour, R. Y. Korotkov, and B. W. Wessels, J. Appl. Phys. **87**, 3351 (2000).
[8] A. Chantre, G. Vincent, and D. Bois, Phys. Rev. B **23**, 5335 (1981).
[9] W. Gebicki, J. Strzeszewski, G. Kamer, T. Szyszko, and S. Podsiadlo, Appl. Phys. Lett **76**, 3870 (2000). Assuming that harmonic approximation holds and the force constants in the ground and excited states of the defect are the same as in the host, the pseudolocal phonon modes were estimated using the simple mass defect approximation. Values of 17.9 and 66 meV were used for the E_2(low) and A_1(TO) phonon modes (Ref. 10), respectively. This approximation is good to within 7% for these mass values as indicated in Ref. 11.
[10] T. Kozawa, T. Kachi, H. Kano, Y. Taga, M. Hashimoto, N. Kode, and K. Manabe, J. Appl. Phys. **75**, 1098 (1994).
[11] A. S. Barker and A. J. Sievers, Rev. Mod. Phys. **47**, 1 (1975).
[12] K. K. Rebane, *Impurity Spectra of Solids* (Plenum, New York, 1970).
[13] Note when the Huang–Rhys parameter is small $S\sim1$, the use of the single-breathing-mode vibration is approximate. As a result, the observed ratio of the sidebands to the ZPL may be much larger than predicted by Eq. (1) (Refs. 12 and 15).
[14] For comparison, the vibrational parameters of the broad PL band at 2.9 eV observed in undoped GaN was shown to couple with pseudolocal and lattice phonons with energies of 36 and 91 meV, respectively (Ref. 7). The Huang–Rhys factors calculated for the pseudolocal and lattice coupling were 1.5 and 2, respectively. The low magnitude of the Huang–Rhys factors indicated that the coupling with pseudolocal phonons is weak ($S\sim1$) for Mn acceptors in GaN (Refs. 12 and 15).
[15] B. Henderson and G. F. Imbusch, *Optical Spectroscopy of Inorganic Solids* (Oxford University, New York, 1989).
[16] R. Y. Korotkov, J. M. Gregie, and B. W. Wessels, Physica B **30**, 308 (2001).
[17] P. M. Mooney, G. A. Northrup, T. N. Morgan, and H. G. Grimmeiss, Phys. Rev. B **37**, 8298 (1988).
[18] P. B. Klein, J. A. Freitas, Jr., S. C. Binari, and A. E. Wickenden, Appl. Phys. Lett. **75**, 4016 (1999).
[19] V. M. Bermudez, J. Appl. Phys. **80**, 1190 (1996).
[20] C. I. Wu and A. Khan, J. Vac. Sci. Technol. B **16**, 2218 (1998).
[21] J. I. Pankove and H. Schade, Appl. Phys. Lett. **25**, 53 (1974).
[22] It is important to note that the behavior of Mn in GaN is very similar to that of Fe^{3+} in GaN (Ref. 23). For example, the lowest intraion transition energy for the $^4T_1(G)-^6A_1(S)$, recombination is 1.25 eV (Ref. 16), which is close to that of Fe^{3+} (Ref. 23). However, Heitz, Hoffmann, and Broser (Ref. 23) indicated that the position of the Fe^{3+} deep level in GaN was inconsistent with VRBE theory. In contrast, our experimental data indicated that Mn forms a deep level in the gap, which is predicted by VRBE theory.
[23] R. Heitz, A. Hoffmann, and I. Broser, Phys. Rev. B **55**, 4382 (1997).
[24] M. van Schlifgaarde and O. N. Mryasov, Phys. Rev. B **63**, 233205 (2001)